

# Exploration of phylogeography of *Monacha cantiana* s.l. continues: the populations of the Apuan Alps (NW Tuscany, Italy) (Eupulmonata, Stylommatophora, Hygromiidae)

Joanna R. Pieńkowska<sup>1</sup>, Giuseppe Manganelli<sup>2</sup>, Folco Giusti<sup>2</sup>, Debora Barbato<sup>2</sup>,  
Alessandro Hallgass<sup>2</sup>, Andrzej Lesicki<sup>1</sup>

**1** Department of Cell Biology, Institute of Experimental Biology, Faculty of Biology, Adam Mickiewicz University in Poznań; Umultowska 89, 61-614 Poznań, Poland **2** Dipartimento di Scienze Fisiche, della Terra e dell'Ambiente, Università di Siena, Via Mattioli 4, 53100 Siena, Italy

Corresponding author: Andrzej Lesicki ([alesicki@amu.edu.pl](mailto:alesicki@amu.edu.pl))

Academic editor: Eike Neubert | Received 12 November 2018 | Accepted 11 December 2018 | Published 9 January 2019

<http://zoobank.org/F76A43CE-D785-409C-A0F8-08D6B1907E8D>

**Citation:** Pieńkowska JR, Manganelli G, Giusti F, Barbato D, Hallgass A, Lesicki A (2019) Exploration of phylogeography of *Monacha cantiana* s.l. continues: the populations of the Apuan Alps (NW Tuscany, Italy) (Eupulmonata, Stylommatophora, Hygromiidae). ZooKeys 814: 115–149. <https://doi.org/10.3897/zookeys.814.31583>

## Abstract

Two new lineages CAN-5 and CAN-6 were recognised in four populations of *Monacha cantiana* (Montagu, 1803) s.l. from the Italian Apuan Alps by joint molecular and morphological analysis. They are different from other *M. cantiana* lineages known from English, Italian, Austrian and French populations, i.e. CAN-1, CAN-2, CAN-3 and CAN-4, as well as from the other Italian *Monacha* species used for comparisons (*M. parumcincta* and *M. cartusiana*). Although a definite taxonomic and nomenclatural setting seems to be premature, we suggest that the name or names for these new lineages as one or two species should be found among 19<sup>th</sup> century names (*Helix sobara* Mabille, 1881, *H. ardesa* Mabille, 1881, *H. apuanica* Mabille, 1881, *H. carfaniensis* De Stefani, 1883 and *H. spallanzanii* De Stefani, 1884).

## Keywords

16SrDNA, COI, H3, ITS2, molecular features, shell and genital structure, species distribution

## Introduction

Study of the phylogeography of the *Monacha cantiana* (Montagu, 1803) s.l. by joint molecular and morphological analysis revealed a number of cryptic lineages, some of which might deserve distinct taxonomic status.

Examination of a first group of English, Italian, Austrian and French populations showed that it consisted of at least four distinct lineages (CAN-1, CAN-2, CAN-3, CAN-4) (Pieńkowska et al. 2018). One of these lineages (CAN-1) included most of the UK (5 sites) and Italian (5 sites) populations examined. Three other lineages were represented by populations from two sites in northern Italy (CAN-2), three sites in northern Italy and Austria (CAN-3) and two sites in south-eastern France (CAN-4). A taxonomic and nomenclatural setting is only currently available for CAN-1 and CAN-4. The lineage CAN-1 corresponds to the true *M. cantiana* (Montagu, 1803) because it is the only one that includes topotypical English populations. The lineage CAN-4 is attributed to *M. cemelelea* (Risso, 1826), for which a neotype has been designated and deposited. A definitive frame for the other two has been postponed because it requires much more research.

We have now studied some populations from the Apuan Alps at the north-western extremity of Tuscany, a well-known hotspot of diversity and endemism (Lanza 1997; Biondi et al. 2013; Garbari and Bedini 2014; Carta et al. 2017; Orsenigo et al. 2018). Molecular study revealed two more lineages (CAN-5 and CAN-6), molecularly distinct from each other and from all the others, but morphologically indistinguishable from each other and only slightly distinguishable from all the other lineages of *M. cantiana*.

## Material and methods

### Taxonomic sample

Four new populations of *Monacha cantiana* s.l. were considered in our analysis of their molecular and morphological (shell and genitalia structure) variability (Table 1) and compared with the other *M. cantiana* lineages (Pieńkowska et al. 2018). The sequences deposited in GenBank were also considered for the molecular analysis. Two other *Monacha* species were used for molecular comparison (*Monacha cartusiana* (Müller, 1774)) and for morphological and molecular comparison (*M. parumcincta* (Rossmässler, 1834)).

### Materials examined

New materials examined are listed as follows, when possible: geographic coordinates of locality, locality (country, region, site, municipality and province), collector(s), date, number of specimens with name of collection where materials are kept in parenthesis (Table 1). The materials are kept in the F. Giusti collection (FGC; Dipartimento di

Scienze Fisiche, della Terra e dell'Ambiente, Università di Siena, Italy). The materials used for comparison have already been described (see Pieńkowska et al. 2018: table 1) and is now supplemented with some new nucleotide sequences (Table 2).

### **DNA extraction, amplification and sequencing**

DNA extraction, amplification and sequencing methods are described in detail in our previous paper (Pieńkowska et al. 2018).

### **Phylogenetic inference**

Two mitochondrial and two nuclear gene fragments were analysed, namely cytochrome c oxidase subunit 1 (COI), 16S ribosomal DNA (16SrDNA), histone 3 (H3) and an internal transcribed spacer of rDNA (ITS2), respectively. All new sequences were deposited in GenBank (Tables 1, 2). The COI, 16SrDNA, H3 and ITS2 sequences obtained from GenBank for comparisons are listed in Table 3.

The sequences were edited by eye using the programme BIOEDIT, version 7.2.6 (Hall 1999). Alignments were performed using CLUSTAL W (Thompson et al. 1994) implemented in MEGA 7 (Kumar et al. 2016). The COI and H3 sequences were aligned according to the translated amino acid sequences. The ends of all sequences were trimmed. The lengths of the sequences after trimming were 591 bp for COI, 355 positions for 16SrDNA, 315 bp for H3 and 496 positions for ITS2. The sequences were collapsed to haplotypes (COI and 16SrDNA) and to common sequences (H3 and ITS2) using the programme ALTER (Alignment Transformation EnviRonment) (Glez-Peña et al. 2010). Gaps and ambiguous positions were removed from alignments prior to phylogenetic analysis. Mitochondrial (COI and 16SrDNA) and nuclear (H3 and ITS2) sequences were combined (Table 4) before phylogenetic analysis. Finally, the sequences of COI, 16SrDNA, H3 and ITS2 were combined (Table 4) for Maximum Likelihood (ML) and Bayesian inference (BI). Before doing so, uncertain regions were removed from 16SrDNA alignment with the GBLOCKS 0.91b (Castresana 2000; Talavera and Castresana 2007) using parameters for relaxed selection of blocks. This procedure shortened 16SrDNA sequences from 355 to 275 positions.

The sequences of COI obtained in this study together with other sequences from GenBank were analysed by the genetic distance Neighbour-Joining method (Saitou and Nei 1987) implemented in MEGA7 using the Kimura two-parameter model (K2P) for pairwise distance calculations (Kimura 1980). Maximum Likelihood (ML) analyses were then performed with MEGA 7. *Monacha cartusiana* and *Monacha parumcincta* were added as outgroup species in each analysis. For ML analysis of combined sequences, the following best nucleotide substitution models were specified according to the Bayesian Information Criterion (BIC): HKY+G (Hasegawa et al. 1985; Kumar et al. 2016) for COI and 16SrDNA combined sequences of 879 positions (591 COI + 288 16SrDNA), TN92+G

**Table 1.** List of localities of the populations of *Monacha cantiana* s.l. (CAN-5 & CAN-6) used for molecular and morphological (SH shell, AN genitalia) research.

No.	Coordinates	Localities		Clade	Revised taxonomy	COI	16SrDNA		H3	ITS2	PCA and RDA	Figs
		Country and site	Collector / date / no. of specimens (collection)				New haplotype (no. spec.)	New common sequence (no. sps)				
1	44°06'54.9"N 10°08'23.9"E	Italy, Tuscany, Apuan Alps, Foce di Pianza (pathway from Campo Cecina to Monte Sagro), 1270 m a.s.l.	A. Hallgass / 13.10.2013 / 5 / (FGC 41565)	CAN-5	<i>M. sp.</i>	COI 1 (4)	16S 1 (4)	MK066929 MK066930 MK066931 MK066932	H3 5 (3)	MK066965 MK066966 MK066967 MK066968	MK066981 MK066982 MK066983 MK066984	8, 9, 25–29
44°05'56.8"N 10°07'08.5"E	Italy, Tuscany, Apuan Alps, Pastra, 290 m a.s.l.	A. Hallgass / 13.10.2013 / 5 / (FGC 41563)	CAN-5	<i>M. sp.</i>	COI 5 (1) COI 1 (3)	16S 7 (1) 16S 8 (1) 16S 6 (1)	MK066955 MK066956 MK066957	H3 7 (1) H3 2 (1) H3 6 (2)	MK066973 MK066974 MK066975 MK066976	MK066989 MK066990 MK066991 MK066992	6, 7, 19–24	
												44°03'25.5"N 10°16'01.0"E

**Table 2.** New ITS2 sequences obtained from the specimens of *Monacha cantiana* s.l. (CAN-2 to CAN-4) and *M. parumcincta* (PAR) used for molecular research. Number of localities after Pieńkowska et al. (2018). Earlier data on other sequences (COI, 16SrDNA, H3 and ITS2) from these localities were published by Pieńkowska et al. (2018).

No.	Coordinates	Localities		Clade	Revised taxonomy	ITS2		
		Country and site	Collector / date / no. of specimens (collection)			New common sequence	No. Spec.	GenBank ##
12	45°11'59.85"N 10°58'49.30"E	Italy, Venetum, Sorgà (Verona)	A. Hallgass / 09.2012 / 6 (FGC 42964)	CAN-2	<i>M. cantiana</i>	ITS2 14	1	MK067000
15	44°22'09.98"N 11°15'11.28"E	Italy, Emilia Romagna, along Fiume Setta, upstream its confluence with Fiume Reno (Sasso Marconi, Bologna)	A. Hallgass / 09.2012 / 3 (FGC 42977)	CAN-3	<i>M. sp.</i>	ITS2 15	1	MK067001
17	48°15'25.50"N 16°30'46.38"E	Austria, Breitenlee, abandoned railway station	M. Duda / 09.2015 / 3 (FGC 44020)	CAN-3	<i>M. sp.</i>	ITS2 16	1	MK067002
18	43°46'11.79"N 07°22'21.50"E	France, Alpes-Maritimes, Vallée de Peillon, Sainte Thecle	A. Hallgass / 24.10.2011/ 5 (FGC 40320)	CAN-4	<i>M. cemelelea</i>	ITS2 17 ITS2 18	1 1	MK067003 MK067004
24	40°13'25.49"N 15°52'17.07"E	Italy, Basilicata, along the road from Moliterno to Fontana d'Eboli (Moliterno, Potenza)	A. Hallgass / 2012 / 5 (FGC 42962)	PAR	<i>M. parumcincta</i>	ITS2 19	1	MK067005

(Tamura 1992; Kumar et al. 2016) for H3+ITS2 combined sequences of 812 positions (315 H3 + 497 ITS2), and GTR+I+G (Nei and Kumar 2000; Kumar et al. 2016) for COI+16SrDNA+H3+ITS2 combined sequences with a total length of 1677 positions (591 COI + 275 16SrDNA + 315 H3 + 496 ITS2). Bayesian analysis was conducted with the MRBAYES 3.1.2 (Ronquist and Huelsenbeck 2003) using the same evolution model as for ML calculation. The GTR substitution model (Nei and Kumar 2000; Kumar et al. 2016), assuming a gamma distributed rate variation (+G) allowing for some sites to be evolutionarily invariable (+I), was identified as the best-fit substitution model using JMODELTEST2 (Darriba et al. 2012). Four Monte Carlo Markov chains were run for one million generations, sampling every 100 generations (the first 250,000 trees were discarded as 'burn-in'). This gave us a 50% majority rule consensus tree. In parallel, Maximum Likelihood (ML) analysis was performed with MEGA7 (Kumar et al. 2016) and calculated bootstrap values were mapped on the 50% majority rule consensus Bayesian tree.

The haplotype network was inferred with NETWORK 5.0.0.1 to reflect all relationships between COI and 16SrDNA haplotypes. During the analysis, a median-joining calculation implemented in NETWORK 5.0.0.1 was used (Bandelt et al. 1999).

### Morphological study

Seventy-eight specimens of seven clades (six lineages of *M. cantiana* s.l.: CAN-1, CAN-2, CAN-3, CAN-4, CAN-5 and CAN-6; one lineage of *M. parumcincta*) were considered for shell variability (see Table 1 and Pieńkowska et al. 2018). Shell variabil-

**Table 3.** GenBank sequences used for comparison in molecular analysis.

Species	COI	16S rDNA	H3	ITS2	References
<i>Monacha cantiana</i> CAN-1	KM247375	KJ458539			Razkin et al. 2015
	KX507234	KM247390			Pienkowska et al. 2015
	MG208884-MG208924	KX495428			Neiber and Hausdorf 2015
<i>Monacha cantiana</i> CAN-2		MG208960-MG208995	MG209031-MG209039	MH137963-MH137978	Pienkowska et al. 2018
		MG208996-MG209004	MG209041-MG209048		
		HQ204502	MG209049-MG209052	MH137979-MH137981	Pienkowska et al. 2018
<i>Monacha cantiana</i> CAN-3		HQ204543		Duda et al. 2011; Kruckenhauser et al. 2014	
<i>Monacha cemenelca</i> CAN-4		KF596907			Cadahia et al. 2014
		MG208933-MG208938	MG209005-MG209010	MH137982-MH137983	Pienkowska et al. 2018
		MG208939-MG208943	MG209011-MG209015		
<i>Monacha</i> sp.		AY741419		MH137984	Pienkowska et al. 2018
<i>Monacha parumincta</i> PAR		AY741418			Manganeli et al. 2005
		MG208944-MG208959	MG209016-MG209030	MH137985-MH137992	Manganeli et al. 2005
<i>Monacha cartusiana</i>		KM247380			Pienkowska et al. 2018
		KX507189			Pienkowska et al. 2015
			MG209072	MH137993	Neiber and Hausdorf 2015
					Pienkowska et al. 2018

ity was analysed randomly choosing five adult specimens from each population, when possible. Twelve shell variables were measured to the nearest 0.1 mm using ADOBE PHOTOSHOP 7.0.1 on digital images of apertural and umbilical standard views taken with a Canon EF 100 mm 1:2.8 L IS USM macro lens mounted on a Canon F6 camera: AH aperture height, AW aperture width, LWfW last whorl final width, LWmW last whorl medial width, LWaH height of adapical sector of last whorl, LWmH height of medial sector of last whorl, PWH penultimate whorl height, PWFw penultimate whorl final width, PwMw penultimate whorl medial width, SD shell diameter, SH shell height, UD umbilicus diameter (see Pieńkowska et al. 2018: fig. 1).

Seventy-five specimens of seven clades (all lineages of *M. cantiana* s.l. plus one lineage of *M. parumcincta*) were analysed for anatomical variability (see Table 1 and Pieńkowska et al. 2018). Snail bodies were dissected under the light microscope (Wild M5A or Zeiss SteREO Lumar V12). Anatomical details were drawn using a Wild camera lucida. Acronyms: BC bursa copulatrix, BW body wall, DBC duct of bursa copulatrix, DG digitiform glands, E epiphallus (from base of flagellum to beginning of penial sheath), F flagellum, FO free oviduct, GA genital atrium, OSD ovispermiduct, P penis, V vagina, VA vaginal appendix (also known as appendicula), VAS vaginal appendix basal sac, VD vas deferens. Six anatomical variables (DBC, E, F, P, V, VA) were measured using a calliper under a light microscope (0.01 mm) (see Pieńkowska et al. 2018: fig. 2).

Detailed methods of multivariate ordination by Principal Component Analysis (PCA) and Redundancy Analysis (RDA), performed on the original shell and genitalia matrices as well as on the Z-matrices (shape-related matrices), are described in a previous paper (Pieńkowska et al. 2018).

Differences between species for each shell and genital character were assessed through box-plots and descriptive statistics. Significance of differences (set at  $p \leq 0.01$ ) was obtained using analysis of variance (ANOVA); when the test proved significant, an adjusted posteriori pair-wise comparison between pairs of species was performed using Tukey's honestly significant difference (HSD) test. All variables were log transformed before analysis.

## Results

### Molecular study

Eighteen sequences of each mitochondrial gene fragment (COI and 16SrDNA) as well as 16 and 25 sequences of nuclear gene fragments (H3 and ITS2, respectively) were deposited in GenBank as MK066929-MK066946 (COI), MK066947-MK066964 (16SrDNA), MK066965-MK066980 (H3) and MK066981-MK067005 (ITS2). Eight COI and 12 16SrDNA haplotypes were recognised among them (Table 1). Eight H3 (Table 1) and 19 ITS2 (Tables 1, 2) common nucleotide sequences were also established. ML trees for combined sequences of mitochondrial COI and 16SrDNA (Fig. 1, Table 4) and of nuclear H3 and ITS2 (Fig. 2, Table 4) gene fragments, as well as the

**Table 4.** Combined Sequences of the following gene sequences: COI+16SrDNA and H3+ITS2 for ML analysis and of COI+16SrDNA+H3+ITS2 for Bayesian analysis.

Combined sequence	COI haplotype	16S haplotype	Combined sequence	H3 sequence	ITS2 sequence	Combined sequence	COI haplotype	16S haplotype	H3 sequence	ITS2 sequence	Locality
IT-COI16S-1	MK066929	MK066947	IT-H3ITS2-6	MK066966	MK066981	IT-CS-1	MK066930	MK066948	MK066966	MK066981	Italy, Tuscany, Foce di Pianza
			IT-H3ITS2-7	MK066967	MK066982	IT-CS-2	MK066931	MK066949	MK066967	MK066982	Italy, Tuscany, Foce di Pianza
			IT-H3ITS2-8	MK066968	MK066983	IT-CS-3	MK066932	MK066950	MK066968	MK066983	Italy, Tuscany, Foce di Pianza
			IT-H3ITS2-13	MK066976	MK066991	IT-CS-4	MK066938	MK066957	MK066976	MK066991	Italy, Piastra
IT-COI16S-2	MK066938	MK066957	IT-CS-5	MK066939	MK066958	IT-CS-5	MK066939	MK066958	MK066977	MK066992	Italy, Piastra
IT-COI16S-3	MK066939	MK066958	IT-CS-6	MK066933	MK066951	IT-CS-6	MK066933	MK066951	MK066969	MK066984	Italy, Piastra
IT-COI16S-4	MK066941	MK066959	IT-H3ITS2-9	MK066970	MK066985	IT-CS-7	MK066934	MK066952	MK066970	MK066985	Italy, Tuscany, Foce di Pianza
IT-COI16S-5	MK066933	MK066951	IT-H3ITS2-11	MK066972	MK066987	IT-CS-8	MK066935	MK066954	MK066972	MK066987	Italy, Tuscany, Campo Cecina
IT-COI16S-6	MK066934	MK066952	IT-H3ITS2-12	MK066973	MK066988	IT-CS-9	MK066936	MK066955	MK066973	MK066988	Italy, Tuscany, Campo Cecina
IT-COI16S-7	MK066935	MK066953	IT-H3ITS2-10	MK066974	MK066989	IT-CS-10	MK066937	MK066956	MK066974	MK066989	Italy, Tuscany, Campo Cecina
IT-COI16S-8	MK066936	MK066954	IT-H3ITS2-4	MK066978	MK066997	IT-CS-11	MK066944	MK066962	MK066978	MK066997	Italy, Tuscany, Campagrina
IT-COI16S-9	MK066937	MK066956	IT-H3ITS2-5	MK066980	MK066999	IT-CS-12	MK066946	MK066964	MK066980	MK066999	Italy, Tuscany, Campagrina
IT-COI16S-10	MK066942	MK066960	UK-H3ITS2-1	MG209031	MH137963	UK-CS-1	MG208884	MG208966	MG209031	MH137963	UK, Barrow near Barnsley
IT-COI16S-11	MK066943	MK066961	UK-H3ITS2-2	MG209038	MH137971	UK-CS-2	MG208899	MG208976	MG209038	MH137971	UK, Rotherham
IT-COI16S-12	MK066944	MK066962	UK-H3ITS2-3	MG209037	MH137969	UK-CS-3	MG208898	MG208975	MG209037	MH137969	UK, Rotherham
IT-COI16S-13	MK066945	MK066963	IT-H3ITS2-15	MG209045	MH137973	IT-CS-13	MG208915	MG208985	MG209045	MH137973	UK, Cambridge
UK-COI16S-1	MG208884	MG208966	IT-H3ITS2-16	MG209046	MH137974	IT-CS-14	MG208916	MG208987	MG209046	MH137974	Italy, Latium, Valle dell'Aniene, Rome
UK-COI16S-2	MG208893	MG208960	IT-H3ITS2-17	MG209047	MH137975	IT-CS-15	MG208917	MG208989	MG209047	MH137975	Italy, Latium, Valle dell'Aniene, Rome
UK-COI16S-3	MG208899	MG208976	IT-H3ITS2-18	MG209039	MH137972	IT-CS-16	MG208905	MG208977	MG209039	MH137972	Italy, Latium, Gole del Velino
UK-COI16S-4	MG208898	MG208975	IT-H3ITS2-19	MG209048	MH137978	IT-CS-17	MG208921	MG208990	MG209048	MH137978	Italy, Latium, Gole del Velino
UK-COI16S-5	MG208891	MG208972	IT-H3ITS2-20	MG209044	MH137978	IT-CS-18	MG208923	MG208994	MG209048	MH137978	Italy, Latium, Valle del Tronto
IT-COI16S-14	MG208915	MG208985	IT-H3ITS2-21	MG209049	MH137979	IT-CS-19	MG208925	MG208996	MG209050	MK067000	Italy, Latium, Valle del Turano
IT-COI16S-15	MG208916	MG208987	IT-H3ITS2-22	MG209050	MK067000	IT-CS-20	MG208926	MG208997	MG209050	MK067000	Italy, Latium, Gole del Velino
IT-COI16S-16	MG208917	MG208989	IT-H3ITS2-23	MG209049	MH137979	IT-CS-21	MG208927	MG208998	MG209050	MK067000	Italy, Venetum, Sorga
IT-COI16S-17	MG208917	MG208989									Italy, Venetum, Sorga
IT-COI16S-18	MG208906	MG208979									Italy, Venetum, Sorga
IT-COI16S-19	MG208921	MG208990									Italy, Venetum, Sorga
IT-COI16S-20	MG208923	MG208994									Italy, Venetum, Sorga
IT-COI16S-21	MG208910	MG208978									Italy, Venetum, Sorga
IT-COI16S-22	MG208925	MG208996									Italy, Venetum, Sorga
IT-COI16S-23	MG208926	MG209001									Italy, Venetum, Sorga
IT-COI16S-24	MG208928	MG208998									Italy, Venetum, Sorga



Combined sequence	COI haplotype	16S haplotype	Combined sequence	H3 sequence	ITS2 sequence	Combined sequence	COI haplotype	16S haplotype	H3 sequence	ITS2 sequence	Locality
IT-COI16S-25	MG208932	MG209003	IT-H3ITS2-20	MG209052	MH137981	IT-CS-20	MG208932	MG209003	MG209052	MH137981	Italy, Lombardy, Rezzato
IT-COI16S-26	MG208934	MG209005	IT-H3ITS2-2	MG209040	MK067001	IT-CS-21	MG208934	MG209005	MG209040	MK067001	Italy, Emilia Romagna, Fiume Setta
IT-COI16S-27	MG208933	MG209007	IT-H3ITS2-3	MG209054	MH137982	IT-CS-22	MG208933	MG209007	MG209054	MH137982	Italy, Emilia Romagna, Fiume Setta
IT-COI16S-28	MG208944	MG209017	IT-H3ITS2-24	MG209061	MK067005	IT-CS-23	MG208944	MG209017	MG209061	MK067005	Italy, Basilicata, Moliterno to Fontana d'Eboli
IT-COI16S-29	MG208946	MG209019	IT-H3ITS2-23	MG209064	MH137992						Italy, Basilicata, Moliterno to Fontana d'Eboli
IT-COI16S-30	MG208949	MG209020				IT-CS-24	MG208949	MG209020	MG209067	MH137987	Italy, Tuscany, Nievole
IT-COI16S-31	MG208950	MG209028	IT-H3ITS2-25	MG209068	MH137989						Italy, Tuscany, Arezzo
			IT-H3ITS2-26	MG209070	MH137990						Italy, Tuscany, Arezzo
			IT-H3ITS2-27	MG209062	MH137986						Italy, Tuscany, Podere Castella
AT-COI16S-1	MG208936	MG209009	AT-H3ITS2-1	MG209055	MH137983	AT-CS-1	MG208936	MG209009	MG209055	MH137983	Austria, Breitenlee
AT-COI16S-2	MG208938	MG209008									Austria, Breitenlee
FR-COI16S-1	MG208939	MG209011	FR-H3ITS2-1	MG209058	MH137984	FR-CS-1	MG208939	MG209011	MG209058	MH137984	France, Sainte Thecle
FR-COI16S-2	MG208940	MG209012	FR-H3ITS2-2	MG209059	MK067003	FR-CS-2	MG208940	MG209012	MG209059	MK067003	France, Sainte Thecle
FR-COI16S-3	MG208941	MG209013	FR-H3ITS2-3	MG209060	MK067004	FR-CS-3	MG208941	MG209013	MG209060	MK067004	France, Sainte Thecle
HU-COI16S-1	KM247376	KM247391	HU-H3ITS2-1	MG209072	MH137993	HU-CS-1	KM247376	KM247391	MG209072	MH137993	Hungary, Kis-Balaton

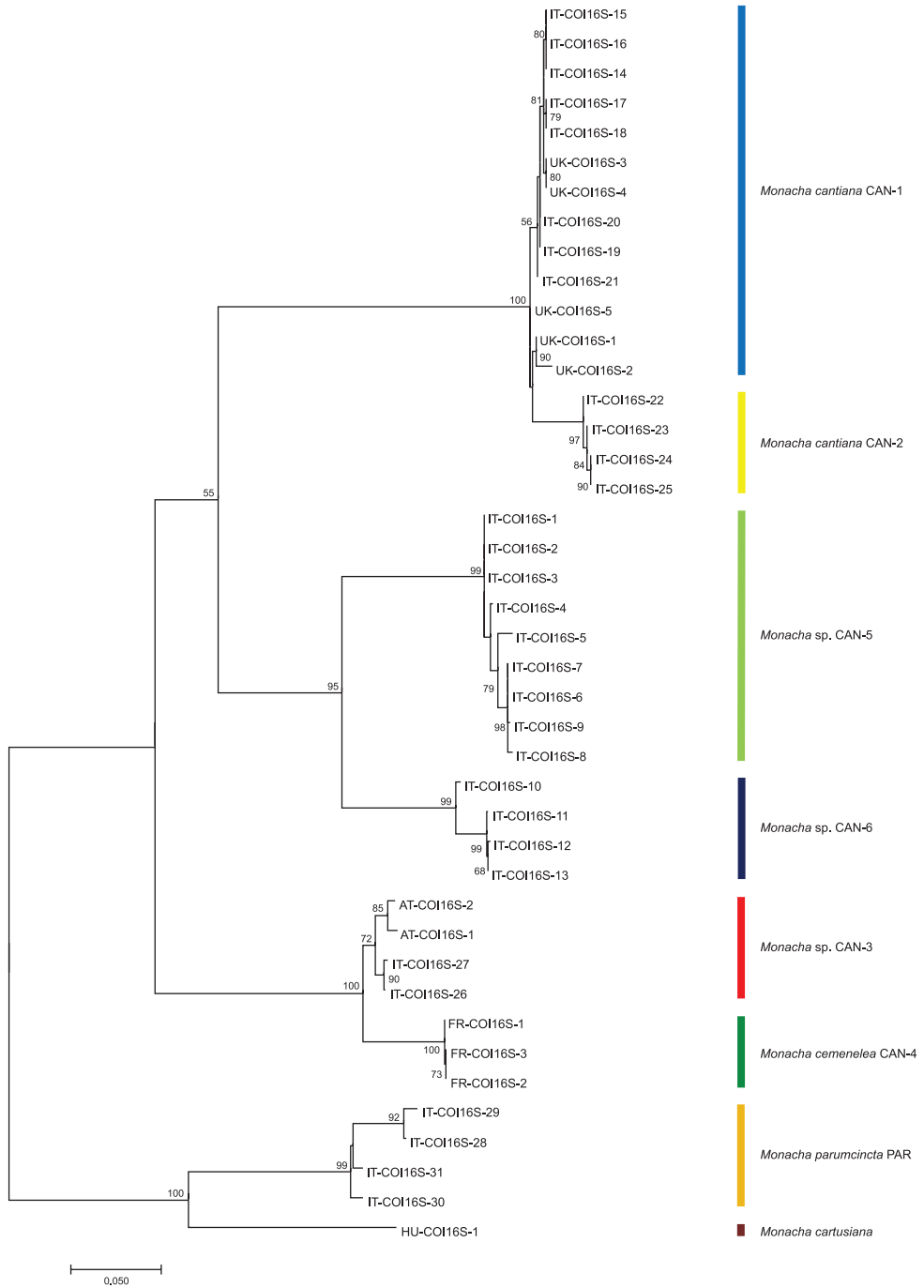


**Figure 1.** Maximum Likelihood (ML) tree of combined COI and 16SrDNA haplotypes of *Monacha cantiana* s.l. (see Table 4). Numbers next to the branches indicate bootstrap support above 50% calculated for 1000 replicates (Felsenstein 1985). The tree was rooted with *M. cartusiana* and *M. parumincta* combined sequences obtained from GenBank (Table 4).

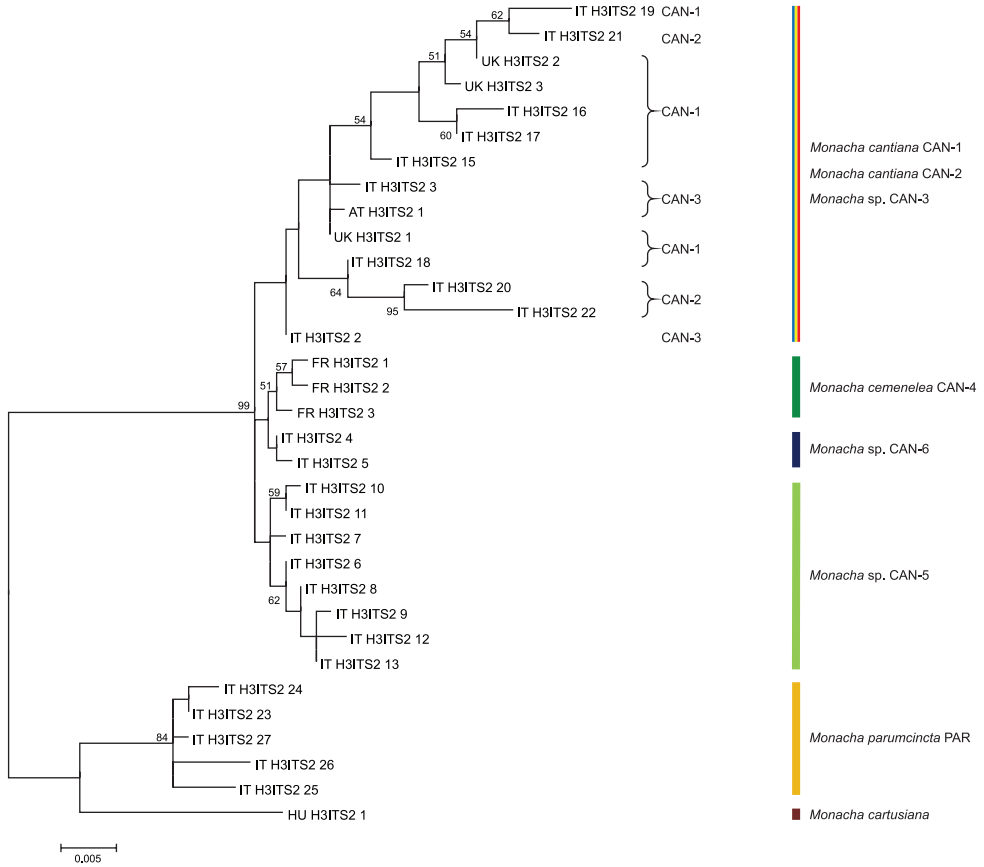


**Figure 2.** Maximum Likelihood (ML) tree of combined H3 and ITS2 common sequences of *Monacha cantiana* s.l. (see Table 4). Numbers next to the branches indicate bootstrap support above 50% calculated for 1000 replicates (Felsenstein 1985). The tree was rooted with *M. cartusiana* and *M. parumcincta* combined sequences obtained from GenBank (Table 4).

Bayesian phylogenetic tree of combined sequences of COI+16SrDNA+H3+ITS2 gene fragments (Fig. 3, Table 4) clustered the combined sequences in two separate clades (CAN-5 and CAN-6), which were also separate from all other clades recognised previously for *M. cantiana* (CAN-1, CAN-2, CAN-3), *M. cemelelea* (CAN-4) and *M. parumcincta* (PAR) populations (Pieńkowska et al. 2018).

Networks of COI (Fig. 4) and 16SrDNA (Fig. 5) confirmed separateness of clades CAN-5 and CAN-6 and all other previously recognised clades (CAN-1 to CAN-4, PAR; Pieńkowska et al. 2018).

K2P genetic distances between COI haplotypes are summarised in Table 5. The smallest distances are within haplotypes of particular clades (0.2–2.2%, slightly larger 1.0–4.2% within *M. parumcincta*). As shown previously (Pieńkowska et al. 2018), the K2P distances between CAN-1 and CAN-2, and between CAN-3 and CAN-4, were smaller (3.3–5.1% and 5.1–6.2%, respectively) than between other clades compared

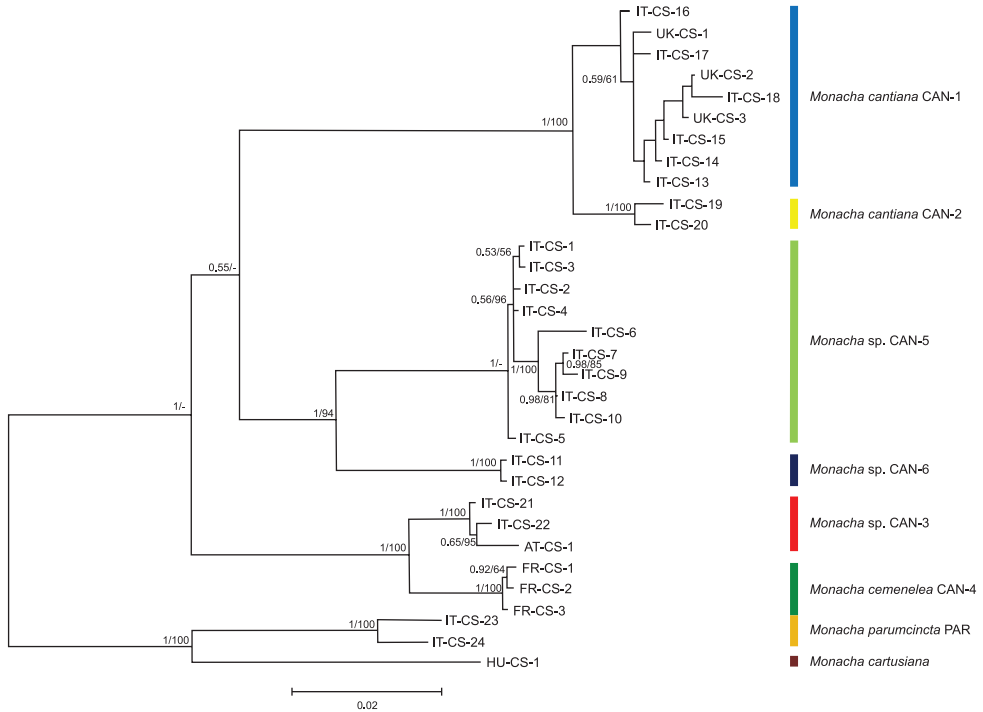


**Figure 3.** Bayesian 50% majority-rule consensus tree of the combined data set of COI and 16S rDNA haplotypes, and H3 and ITS2 common sequences (see Table 4). Posterior probabilities (left) and bootstrap support above 50% from ML analysis (right) are indicated next to the branches. Bootstrap analysis was run with 1000 replicates (Felsenstein 1985). The tree was rooted with *M. cartusiana* and *M. parumincta* combined sequences obtained from GenBank (Table 4).

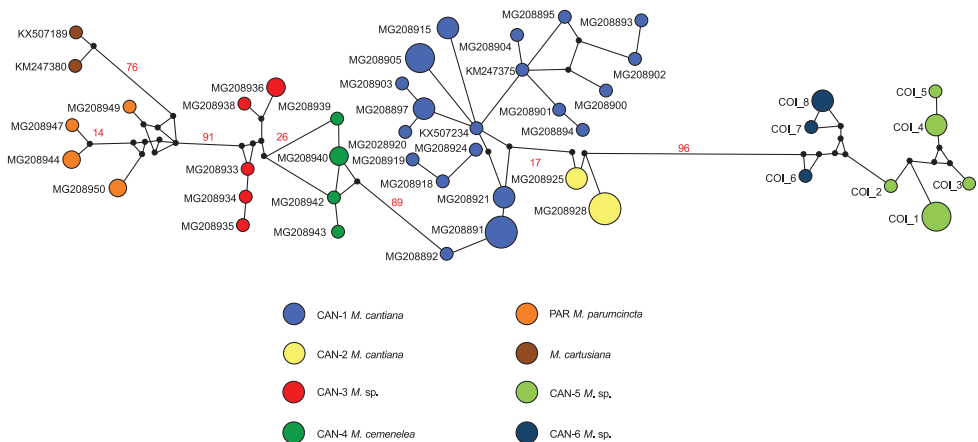


**Figure 4.** The median-joining haplotype network for COI haplotypes of *Monacha cantiana* s.l. The colours of the circles indicate *Monacha* species, and their size is proportional to haplotype frequencies. Small black circles are hypothetical missing intermediates. The numbers next to the branches indicate distance between taxa expressed in numbers of mutant positions. Only numbers above 10 are indicated.

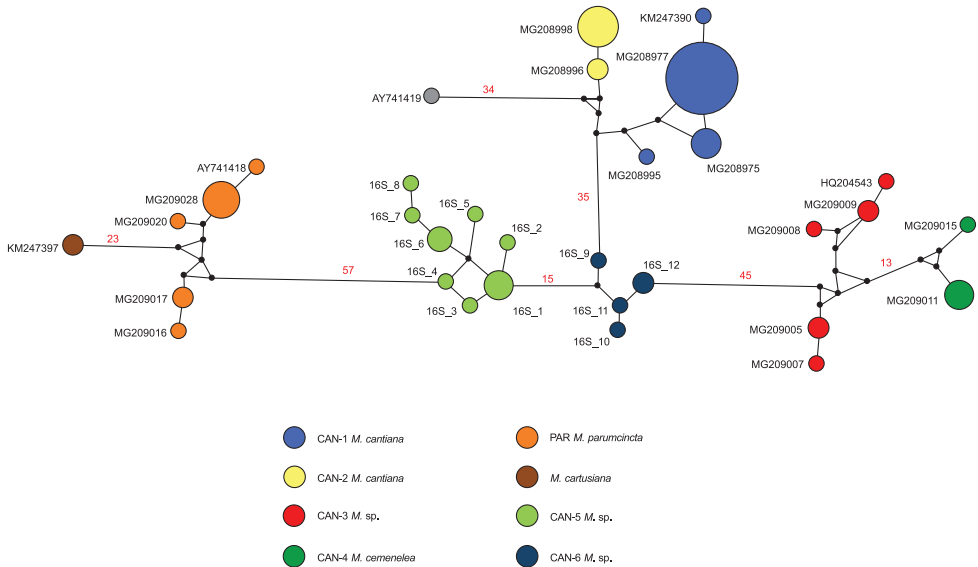


**Figure 5.** Haplotype network for 16SrDNA of *Monacha cantiana* s.l. Other explanations as in Figure 4.

in pairs (Table 5). The clades CAN-5 and CAN-6 differed considerably (12.4–14.3%). The clade CAN-5 differed to a similar degree from CAN-3 and CAN-4 clades (13.3–15.4%). Differences between these two clades (CAN-3 and CAN-4) and the clade CAN-6 were even larger (14.3–16.8%). Both CAN-5 and CAN-6 were also separated by very large genetic distances from all other clades (16.5–21.3%).

### Morphological study: shell

The two new clades of *M. cantiana* s.l. (CAN-5, CAN-6: Figs 6–15) have a globose-subglobose shell, variable in size and usually whitish or pale yellowish, with slightly descending, roundish to oval aperture, very similar to those of the other lineages (CAN-1, CAN-2, CAN-3, CAN-4; see Pieńkowska et al. 2018: figs 8–15), but clearly distinguished by a larger, very open umbilicus.

*M. cantiana* s.l. (lineages CAN-1 to CAN-6) is always distinguished from *M. parumcinata* by its umbilicus (open in *M. cantiana* s.l.; closed in *M. parumcinata*). Some populations of *M. parumcinata* have variably evident whitish peripheral and subsutural bands (evident if the last whorl is reddish) and/or a less glossy (more opaque) shell surface.

RDA with lineage constraint on the shape and size matrix (Fig. 16) showed that RDA 1 (44%,  $p < 0.001$ ) separated the groups CAN-1, CAN-2, CAN-3, CAN-4, CAN-5 and CAN-6 from PAR. The preliminary classic PCA revealed size as the first major source of morphological variation, since PC1 (74%) was a positive combination of all variables. On the contrary, RDA 2 (7%,  $p < 0.01$ ) separated CAN-1, CAN-2 and CAN-3 from CAN-4, CAN-5 and CAN-6 with PAR in intermediate position. In this regard, PC2 (11%) accounted for a contrast between LWmH vs LWaH and PWH variables.

**Table 5.** Ranges of K2P genetic distances for COI sequences analysed (mean values in parentheses).

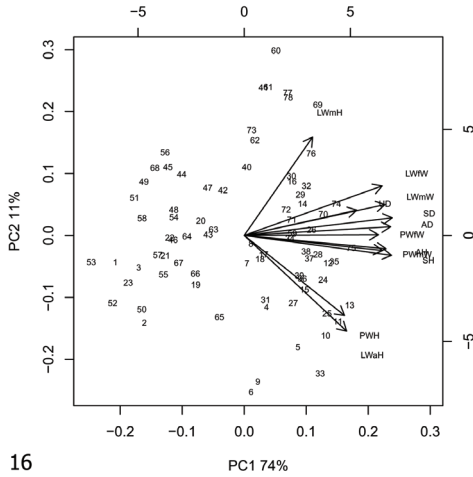
Comparison	COI (%)
Within <i>M. cantiana</i> CAN-1	0.2–2.2 (0.8)
Within <i>M. cantiana</i> CAN-2	0.3 (0.3)
Within <i>M. sp.</i> CAN-3	0.2–1.9 (1.2)
Within <i>M. cemelelea</i> CAN-4	0.2–0.5 (0.3)
Within <i>M. sp.</i> CAN-5	0.2–1.7 (1.3)
Within <i>M. sp.</i> CAN-6	0.2–2.2 (1.6)
Within <i>M. parumcincta</i>	1.0–4.2 (3.0)
Within <i>M. cartusiana</i>	0.5
Between <i>M. cantiana</i> CAN-1 and <i>M. cantiana</i> CAN-2	3.3–5.1 (3.9)
Between <i>M. cantiana</i> CAN-1 and <i>M. sp.</i> CAN-3	17.6–19.2 (18.6)
Between <i>M. cantiana</i> CAN-1 and <i>M. cemelelea</i> CAN-4	17.2–18.7 (18.0)
Between <i>M. cantiana</i> CAN-1 and <i>M. sp.</i> CAN-5	16.5–18.2 (17.5)
Between <i>M. cantiana</i> CAN-1 and <i>M. sp.</i> CAN-6	18.0–19.2 (18.6)
Between <i>M. cantiana</i> CAN-1 and <i>M. parumcincta</i>	19.6–21.7 (20.7)
Between <i>M. cantiana</i> CAN-1 and <i>M. cartusiana</i>	18.9–20.5 (19.7)
Between <i>M. cantiana</i> CAN-2 and <i>M. sp.</i> CAN-3	17.8–18.2 (18.1)
Between <i>M. cantiana</i> CAN-2 and <i>M. cemelelea</i> CAN-4	18.2–18.7 (18.5)
Between <i>M. cantiana</i> CAN-2 and <i>M. sp.</i> CAN-5	17.6–18.2 (17.9)
Between <i>M. cantiana</i> CAN-2 and <i>M. sp.</i> CAN-6	18.3–19.0 (18.5)
Between <i>M. cantiana</i> CAN-2 and <i>M. parumcincta</i>	19.8–20.7 (20.2)
Between <i>M. cantiana</i> CAN-2 and <i>M. cartusiana</i>	21.4
Between <i>M. sp.</i> CAN-3 and <i>M. cemelelea</i> CAN-4	5.1–6.2 (5.6)
Between <i>M. sp.</i> CAN-3 and <i>M. sp.</i> CAN-5	13.3–14.4 (13.8)
Between <i>M. sp.</i> CAN-3 and <i>M. sp.</i> CAN-6	14.3–16.7 (15.7)
Between <i>M. sp.</i> CAN-3 and <i>M. parumcincta</i>	18.4–21.4 (19.6)
Between <i>M. sp.</i> CAN-3 and <i>M. cartusiana</i>	18.4–20.0 (19.1)
Between <i>M. cemelelea</i> CAN-4 and <i>M. sp.</i> CAN-5	14.8–15.4 (15.1)
Between <i>M. cemelelea</i> CAN-4 and <i>M. sp.</i> CAN-6	16.4–16.8 (16.6)
Between <i>M. cemelelea</i> CAN-4 and <i>M. parumcincta</i>	19.5–20.5 (19.9)
Between <i>M. cemelelea</i> CAN-4 and <i>M. cartusiana</i>	18.9–19.3 (19.0)
Between <i>M. sp.</i> CAN-5 and <i>M. sp.</i> CAN-6	12.4–14.3 (13.6)
Between <i>M. sp.</i> CAN-5 and <i>M. parumcincta</i>	17.3–20.2 (18.5)
Between <i>M. sp.</i> CAN-5 and <i>M. cartusiana</i>	20.6–21.3 (21.1)
Between <i>M. sp.</i> CAN-6 and <i>M. parumcincta</i>	17.6–19.1 (18.2)
Between <i>M. sp.</i> CAN-6 and <i>M. cartusiana</i>	17.3–17.8 (17.5)

RDA on the shape (Z) matrix (Fig. 17) showed no separation of lineages, confirming that size is a major source of morphological variation. Shape-related PCA indicated that LWfW and LWmW vs SH, LWaH and PWH were the two principal shape determinants on PC1 and AD vs UD on PC2.

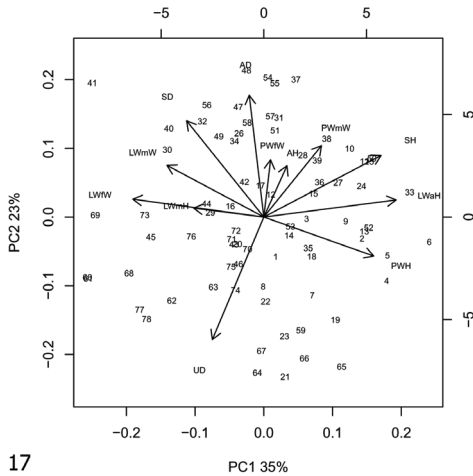
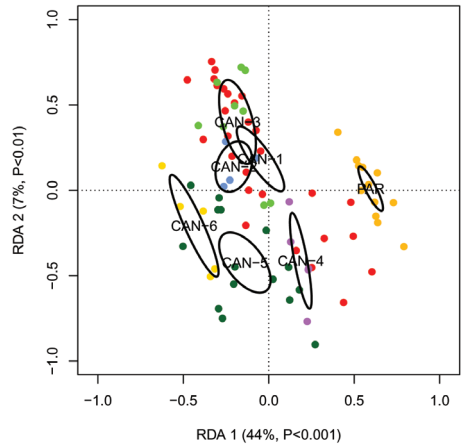
Box plots (Fig. 18) proved the poor discriminating value of shell characters in distinguishing lineage pairs. The best discriminant character was UD that distinguished 13 clade pairs according to Tukey's honestly significant difference test, followed by LWmH and LWmW that distinguished seven clade pairs each. The most recognizable pairs were CAN-1 vs PAR, CAN-3 vs PAR, CAN-6 vs PAR, CAN-2 vs PAR and CAN-5 vs PAR (12, 11, 10, 8 and 7 significant characters, respectively). Five significant shell characters distinguished CAN-3 vs CAN-4, four CAN-4 vs CAN-6, two CAN-1 vs CAN-4, CAN-1 vs CAN-5 or CAN-3 vs CAN-5 and only one CAN-1 vs



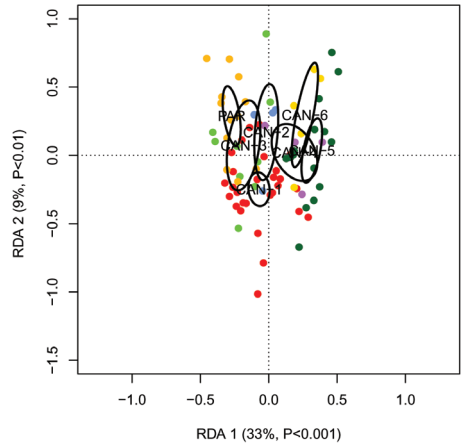
**Figures 6–15.** Shell variability in *Monacha cantiana* s.l. CAN-5 from Piastra (FGC 41563) (**6, 7**), Foce di Pianza (FGC 41565) (**8, 9**) and Campo Cecina (FGC 41564) (**10–12**); CAN-6 from Campagrina (FGC 40322) (**13–15**).



16



17



**Figures 16, 17.** Principal component analysis (PCA) and Redundancy analysis (RDA) with lineage constraint applied to the original shell matrix (**16**) and Z-matrix (shape-related) (**17**).

CAN-6, CAN-2 vs CAN-6, CAN-3 vs CAN-6, CAN-4 vs CAN-5 or CAN-4 vs PAR. No significant character distinguished CAN-1 vs CAN-2, CAN-1 vs CAN-3, CAN-2 vs CAN-3, CAN-2 vs CAN-4, CAN-2 vs CAN-5 or CAN-5 vs CAN-6 (Table 6).

### Morphological study: anatomy

The bodies (generally pinkish or yellowish white) and mantle (with sparse brown or blackish spots near the mantle border or on the lung surface, a larger one close to the pneumostomal opening) of CAN-5 and CAN-6 are very similar to those of the other lineages of *M. cantiana* s.l. and *M. parumcincta* studied so far (Pieńkowska et al. 2018). The



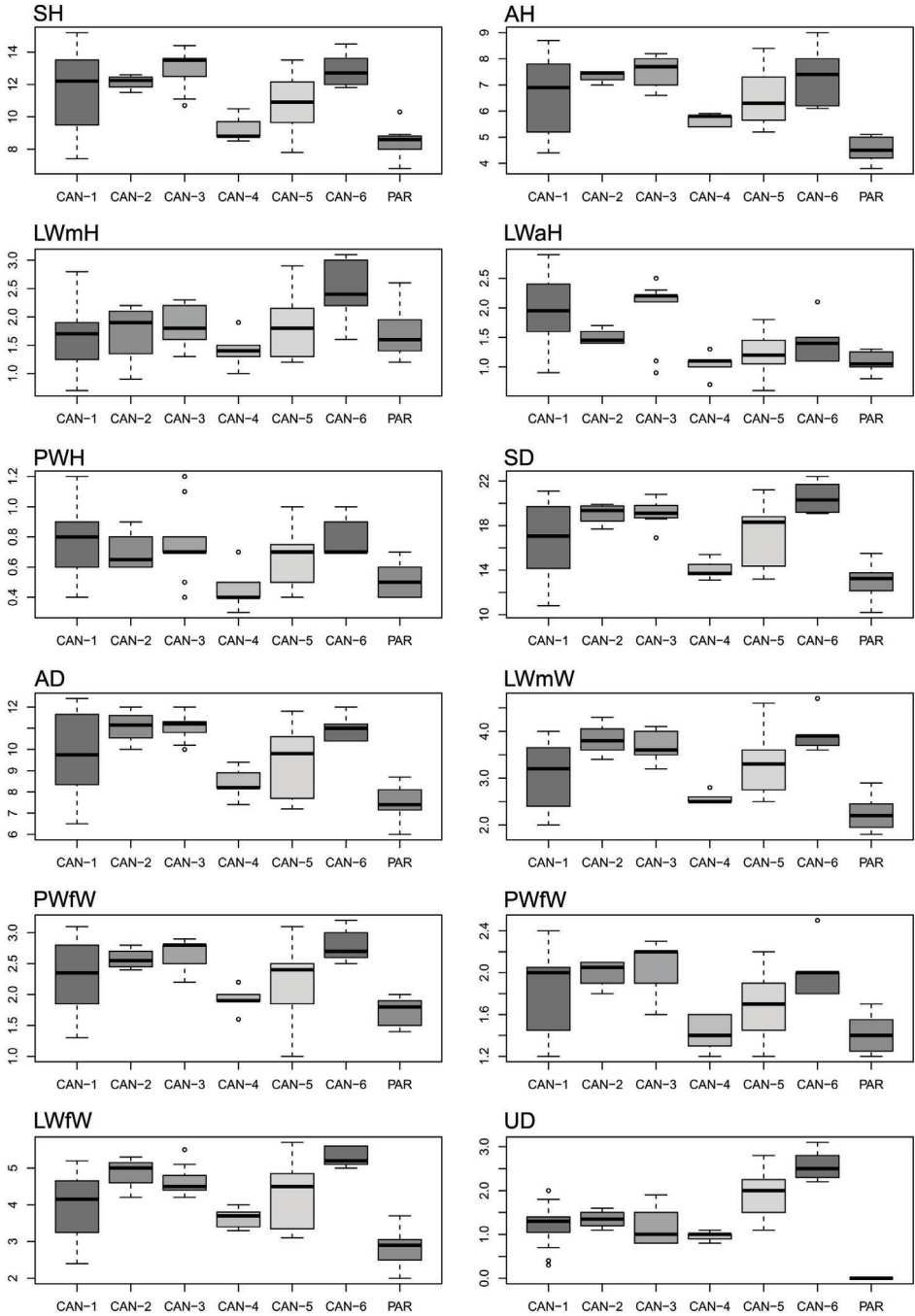
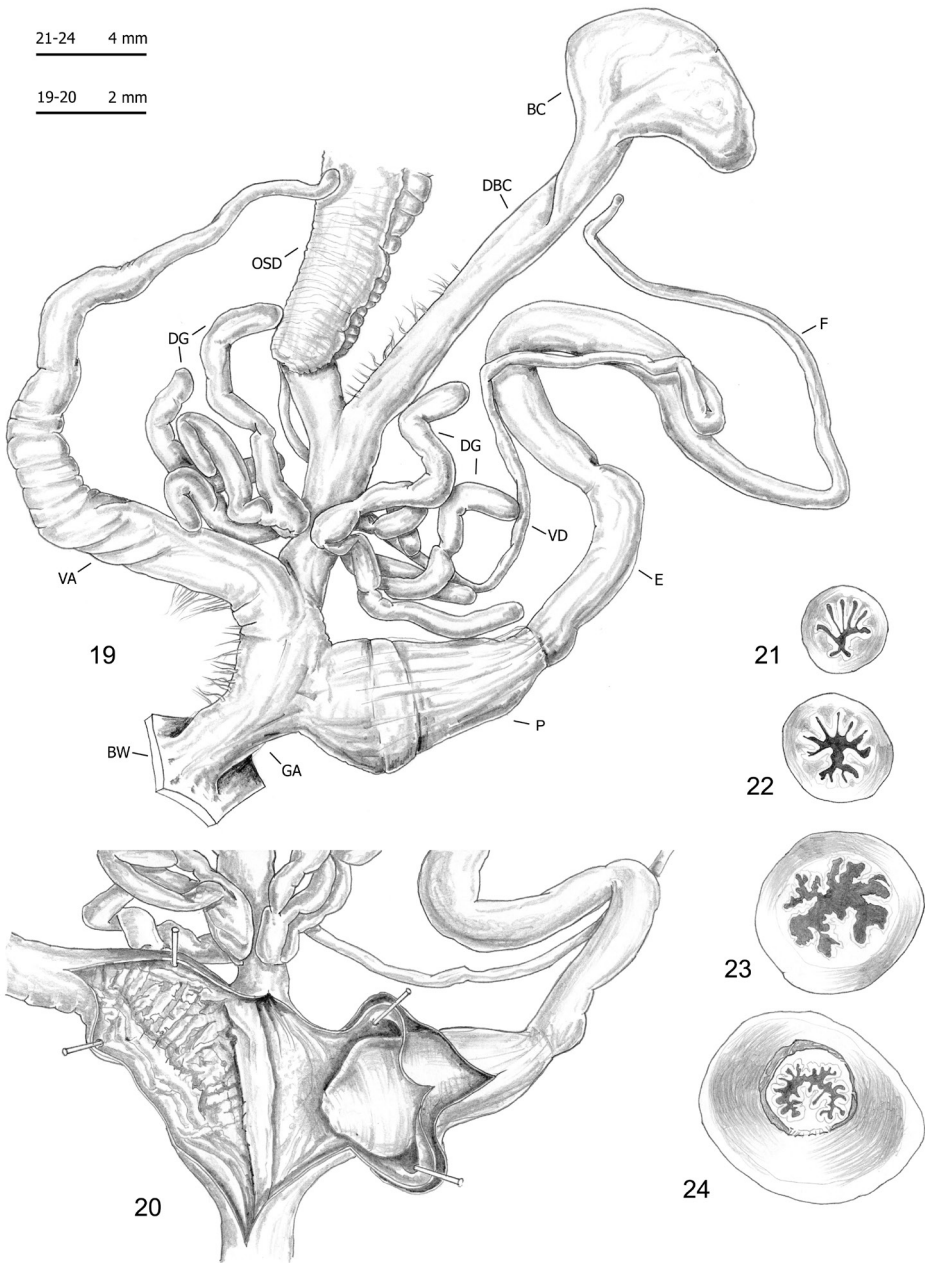


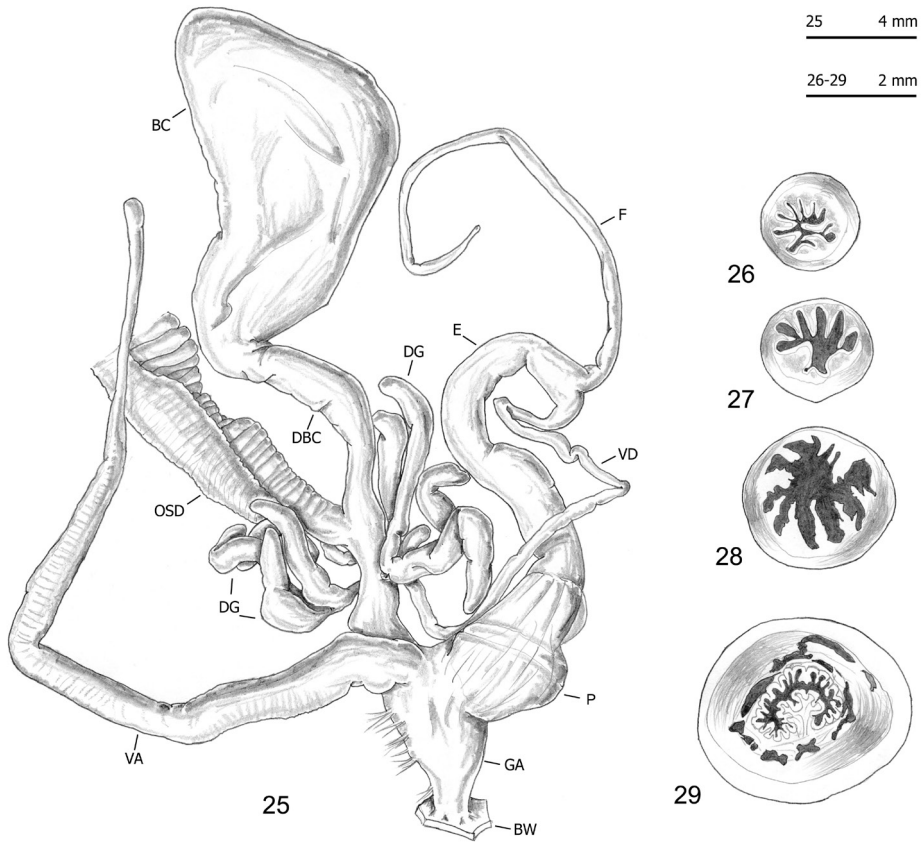
**Figure 18.** Box plots for shell characters of the seven *Monacha* clades investigated. The lower and upper limits of the rectangular boxes indicate the 25<sup>th</sup> to 75<sup>th</sup> percentile range, and the horizontal line within the boxes is the median (50<sup>th</sup> percentile).

**Table 6.** Results of Tukey's honestly significant difference (HSD) test for shell and genitalia characters (in bold Tukey's post-hoc  $p \leq 0.01$ ).

Pairs	SH	AH	LWmH	LWwH	PWH	SD
CAN-1 vs CAN-2	0.99624	0.80619	0.13492	0.64537	0.99057	0.63122
CAN-1 vs CAN-3	0.52140	0.28168	0.06284	1.00000	0.99999	0.22745
CAN-1 vs CAN-4	0.08096	0.59307	0.54497	<b>0.00097</b>	<b>0.00582</b>	0.34307
CAN-1 vs CAN-5	0.81752	0.99959	0.86439	<b>0.00006</b>	0.44707	0.99988
CAN-1 vs CAN-6	0.77627	0.80465	0.02347	0.29268	0.99992	0.08726
CAN-1 vs PAR	<b>0.00001</b>	<b>0.00000</b>	<b>0.00009</b>	<b>0.00001</b>	<b>0.00125</b>	<b>0.00032</b>
CAN-2 vs CAN-3	0.99544	0.99999	0.99929	0.77166	0.99881	1.00000
CAN-2 vs CAN-4	0.15929	0.22915	0.01822	0.55297	0.33334	0.07297
CAN-2 vs CAN-5	0.82169	0.71176	0.57227	0.84890	0.99950	0.79654
CAN-2 vs CAN-6	0.99776	1.00000	0.99993	0.99994	0.98407	0.99242
CAN-2 vs PAR	<b>0.00365</b>	<b>0.00008</b>	<b>0.00002</b>	0.51420	0.51214	<b>0.00095</b>
CAN-3 vs CAN-4	<b>0.00643</b>	0.04670	<b>0.01004</b>	<b>0.00675</b>	0.03910	0.01412
CAN-3 vs CAN-5	0.10929	0.23103	0.60853	<b>0.00526</b>	0.85885	0.48747
CAN-3 vs CAN-6	1.00000	0.99988	0.97726	0.47647	0.99950	0.98207
CAN-3 vs PAR	<b>0.00000</b>	<b>0.00000</b>	<b>0.00000</b>	<b>0.00068</b>	0.04033	<b>0.00001</b>
CAN-4 vs CAN-5	0.53531	0.81117	0.17929	0.96835	0.24318	0.30059
CAN-4 vs CAN-6	0.02495	0.21289	<b>0.00350</b>	0.68422	0.03827	<b>0.00540</b>
CAN-4 vs PAR	0.94161	0.19901	0.70423	0.99998	0.99243	0.94050
CAN-5 vs CAN-6	0.30662	0.70539	0.24510	0.94331	0.73973	0.19886
CAN-5 vs PAR	<b>0.00429</b>	<b>0.00004</b>	<b>0.00001</b>	0.97460	0.33336	<b>0.00072</b>
CAN-6 vs PAR	<b>0.00009</b>	<b>0.00003</b>	<b>0.00000</b>	0.65314	0.05065	<b>0.00001</b>
Pairs	AD	LWmW	PWmW	PWfW	LWfW	UD
CAN-1 vs CAN-2	0.69737	0.13492	0.93036	0.87269	0.31096	0.96096
CAN-1 vs CAN-3	0.31086	0.06284	0.60648	0.41696	0.21613	0.99999
CAN-1 vs CAN-4	0.50802	0.54497	0.09498	0.68052	0.97680	0.88793
CAN-1 vs CAN-5	0.96922	0.86439	0.80483	0.97841	0.92956	<b>0.00001</b>
CAN-1 vs CAN-6	0.64832	0.02347	0.86310	0.28589	0.01739	<b>0.00000</b>
CAN-1 vs PAR	<b>0.00015</b>	<b>0.00009</b>	<b>0.00253</b>	<b>0.00752</b>	<b>0.00003</b>	<b>0.00000</b>
CAN-2 vs CAN-3	1.00000	0.99929	1.00000	1.00000	0.99951	0.95368
CAN-2 vs CAN-4	0.13909	0.01822	0.07501	0.33305	0.22490	0.65706
CAN-2 vs CAN-5	0.41336	0.57227	0.53801	0.63842	0.76317	0.27349
CAN-2 vs CAN-6	1.00000	0.99993	1.00000	0.99559	0.99073	<b>0.00493</b>
CAN-2 vs PAR	<b>0.00086</b>	<b>0.00002</b>	0.01749	0.02031	<b>0.00004</b>	<b>0.00000</b>
CAN-3 vs CAN-4	0.03838	<b>0.01004</b>	<b>0.01014</b>	0.09468	0.21544	0.97116
CAN-3 vs CAN-5	0.11621	0.60853	0.13645	0.18479	0.82554	<b>0.00061</b>
CAN-3 vs CAN-6	1.00000	0.97726	1.00000	0.99741	0.83628	<b>0.00001</b>
CAN-3 vs PAR	<b>0.00001</b>	<b>0.00000</b>	<b>0.00029</b>	<b>0.00030</b>	<b>0.00000</b>	<b>0.00000</b>
CAN-4 vs CAN-5	0.89567	0.17929	0.58669	0.95667	0.75219	<b>0.00034</b>
CAN-4 vs CAN-6	0.11242	<b>0.00350</b>	0.04140	0.06153	0.02534	<b>0.00000</b>
CAN-4 vs PAR	0.78586	0.70423	1.00000	0.96612	0.13925	<b>0.00000</b>
CAN-5 vs CAN-6	0.35200	0.24510	0.38979	0.13051	0.16182	0.17535
CAN-5 vs PAR	0.01180	<b>0.00001</b>	0.19674	0.14546	<b>0.00001</b>	<b>0.00000</b>
CAN-6 vs PAR	<b>0.00030</b>	<b>0.00000</b>	<b>0.00588</b>	<b>0.00062</b>	<b>0.00000</b>	<b>0.00000</b>
Pairs	DBC	V	F	E	P	VA
CAN-1 vs CAN-2	0.07018	0.99978	0.78435	0.11949	0.17040	<b>0.00083</b>
CAN-1 vs CAN-3	0.95915	0.99932	0.98006	0.74183	0.08763	0.23114
CAN-1 vs CAN-4	0.99996	0.63222	0.22100	0.81959	0.76747	0.89555
CAN-1 vs CAN-5	0.94079	0.99983	<b>0.00000</b>	0.23792	0.98466	0.98588
CAN-1 vs CAN-6	0.21936	0.02524	<b>0.00000</b>	0.84359	1.00000	0.13261
CAN-1 vs PAR	0.95468	<b>0.00603</b>	0.01845	<b>0.00032</b>	0.98841	<b>0.00000</b>
CAN-2 vs CAN-3	0.59703	0.99388	0.99743	0.91922	1.00000	0.48744
CAN-2 vs CAN-4	0.22526	0.62669	0.04688	0.04004	0.04443	0.29982
CAN-2 vs CAN-5	0.01390	0.99642	<b>0.00000</b>	0.98147	0.55615	<b>0.00027</b>
CAN-2 vs CAN-6	1.00000	0.04898	<b>0.00000</b>	0.97601	0.52105	0.95169
CAN-2 vs PAR	0.02181	0.16528	0.84806	<b>0.00000</b>	0.08682	<b>0.00000</b>
CAN-3 vs CAN-4	0.96675	0.90393	0.11396	0.27618	0.02653	0.99623
CAN-3 vs CAN-5	0.60068	1.00000	<b>0.00000</b>	0.99937	0.42618	0.08653
CAN-3 vs CAN-6	0.78328	0.14420	<b>0.00000</b>	1.00000	0.43860	0.99411
CAN-3 vs PAR	0.64853	0.01508	0.39875	<b>0.00006</b>	0.04538	<b>0.00000</b>
CAN-4 vs CAN-5	0.99962	0.81255	<b>0.00036</b>	0.08838	0.48386	0.65711
CAN-4 vs CAN-6	0.37610	0.86820	<b>0.00508</b>	0.37200	0.91204	0.91815
CAN-4 vs PAR	0.99956	<b>0.00208</b>	<b>0.00054</b>	0.48361	0.98179	<b>0.00000</b>
CAN-5 vs CAN-6	0.06177	0.06806	1.00000	0.99998	0.99871	0.05266
CAN-5 vs PAR	1.00000	<b>0.00588</b>	<b>0.00000</b>	<b>0.00000</b>	0.82000	<b>0.00000</b>
CAN-6 vs PAR	0.07869	<b>0.00001</b>	<b>0.00000</b>	<b>0.00088</b>	0.99850	<b>0.00000</b>



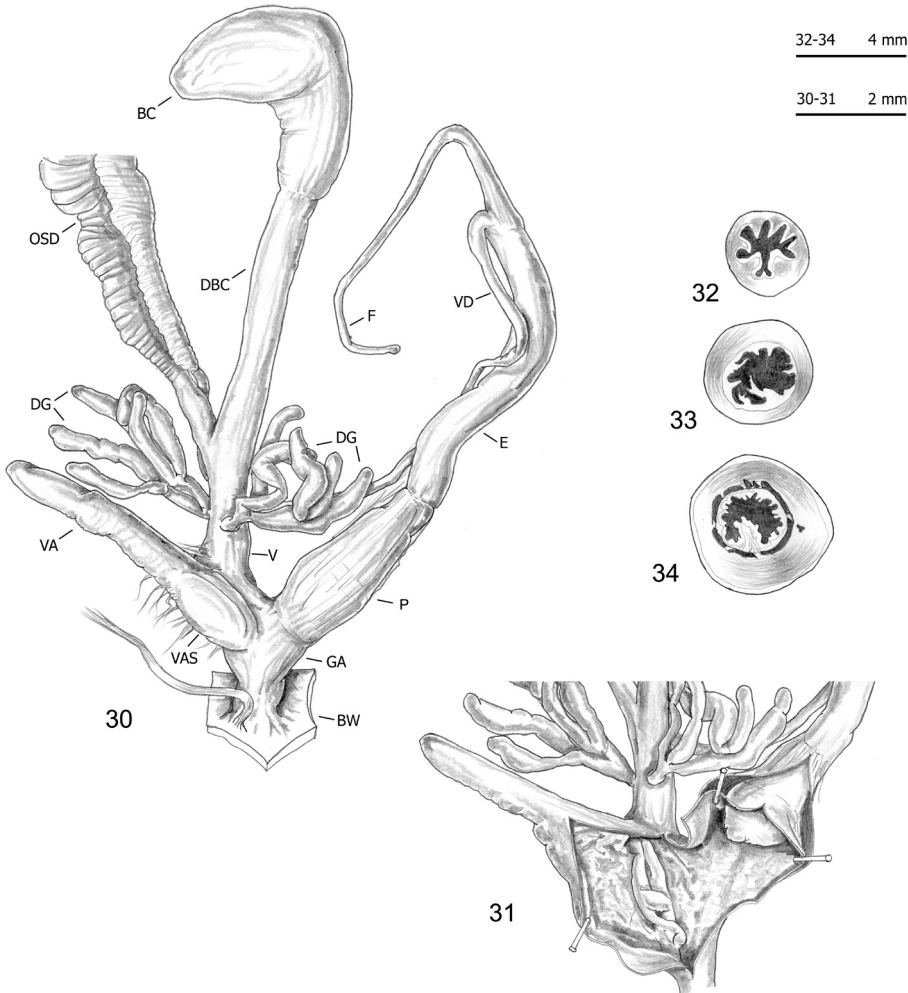
**Figures 19–24.** Genitalia (proximal parts excluded) (19), internal structure of distal genitalia (20), transverse sections of medial epiphallus (21, 22) and basal and apical penial papilla (23, 24) of *Monacha cantiana* s.l. CAN-5 from Piastra (FGC 41563).



**Figures 25–29.** Genitalia (proximal parts excluded) (**25**), internal structure of distal genitalia (**26**), transverse sections of medial epiphallus (**27**) and basal and apical penial papilla (**28, 29**) of *Monacha cantiana* s.l. CAN-5 from Foce di Pianza (FGC 41565).

same is true of the distal genitalia (CAN-5: Figs 19–34; CAN-6: Figs 35–41), which as in the other lineages, have vaginal appendix (or “appendicula”) rather long, always with thin walled terminal portion and with variably evident basal sac; vaginal-atrial pilaster variably evident; epiphallus section with five to six small pleats on one side, two large pleats on the opposite side and, between them, a very small pleat; penial papilla (or glans) section with central canal wide, thin walled, internally irregularly jagged and with a sort of solid pilaster on one side; central canal connected to external wall of penial papilla by many muscular/connective strings as in the other lineages (Pienkowska et al. 2018).

*M. cantiana* s.l. (lineages CAN-1 to CAN-6) is always distinguished from *M. parumcincta* by its vaginal appendix (rather long with thin-walled terminal portion and variably evident basal sac in *M. cantiana*; short, only occasionally with very short terminal portion and always without basal sac in *M. parumcincta*); vaginal-atrial pilaster (present and variably evident in *M. cantiana* s.l.; absent in *M. parumcincta*); penial papilla (central canal connected to external wall by many muscular/connective strings,

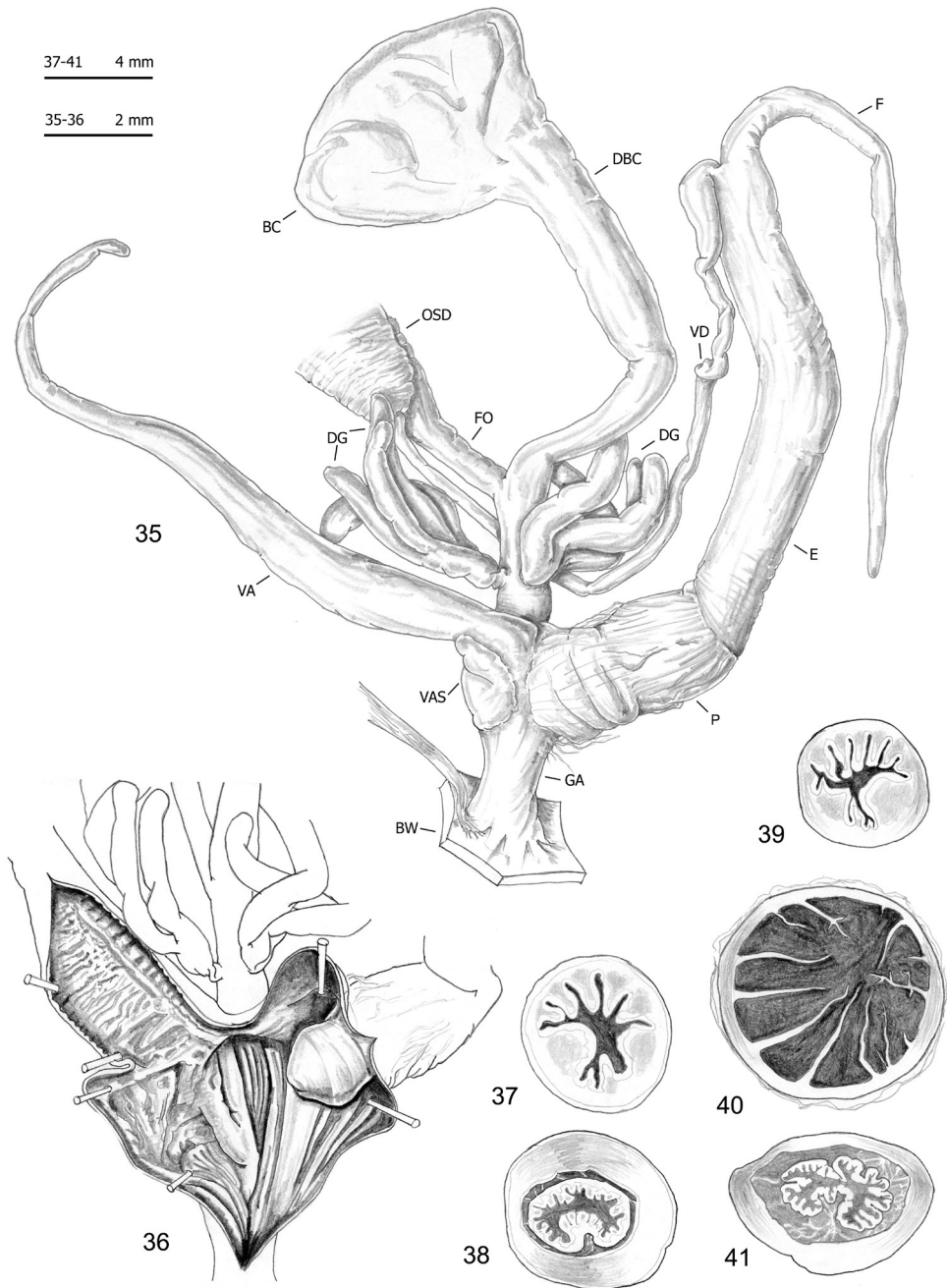


**Figures 30–34.** Genitalia (proximal parts excluded) (30), transverse sections of medial epiphallus (31, 32) and basal and apical penial papilla (33, 34) of *Monacha cantiana* s.l. CAN-5 Campo Cecina (FGC 41564).

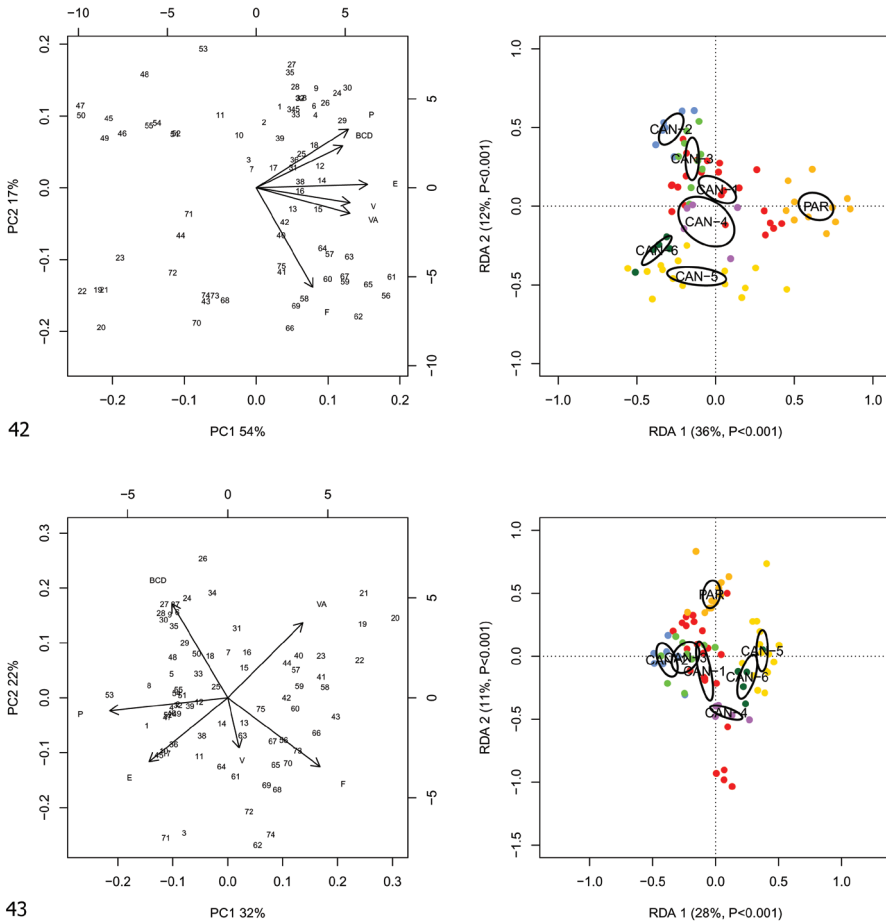
internally jagged and with a sort of solid pilaster on one side in *M. cantiana* s.l.; central canal not connected to external wall, internally smooth or slightly jagged and almost completely filled by large invagination in *M. parumcincta*).

RDA with lineage constraint on the shape and size matrix (Fig. 42) showed that RDA 1 (36%,  $p < 0.001$ ) separated the *M. cantiana* s.l. (CAN-1, CAN-2, CAN-3, CAN-4, CAN-5 and CAN-6) from PAR. The preliminary classic PCA revealed size as the first major source of morphological variation, since PC1 (54%) was a positive combination of all variables. On the contrary, RDA 2 (12%,  $p < 0.001$ ) separated the group CAN-1, CAN-2, CAN-3, CAN-4 and PAR from the group CAN-5 and CAN-6. In that regard, PC2 (17%) accounted for a contrast between P and DBC vs F.





**Figures 35–41.** Genitalia (proximal parts excluded) (35), internal structure of distal genitalia (36) and transverse sections of medial epiphallus (37, 39), basal and apical penial papilla (38, 40, 41) of *Monacha cantiana* s.l. CAN-6 from Campagrina (FGC 40322).



**Figures 42, 43.** Principal component analysis (PCA) and Redundancy analysis (RDA) with lineage applied to the original genitalia matrix (42) and Z-matrix (shape-related) (43).

RDA with species constraint on the shape (Z) matrix (Fig. 43) showed that RDA 1 (28%,  $p < 0.001$ ) separated the group CAN-1, CAN-2 and CAN-3 from the group CAN-5 and CAN-6 with PAR and CAN-4 in intermediate position and that RDA 2 (11%,  $p < 0.001$ ) separated PAR from CAN-4 with the large group CAN-1, CAN-2, CAN-3, CAN-5 and CAN-6 in intermediate position. Shape-related PCA indicated that P, E and DBC vs VA and F were the two principal shape determinants on PC1 and DBC and VA vs E, V and F on PC2. In the latter case, removing the size effect altered the overall relationship patterns.

Box plots (Fig. 44) for anatomical characters showed that F and VA have the best discriminating value (they distinguished 11 and 8 clade pairs, respectively, according to Tukey's honestly significant difference test), followed by E and V (five and four

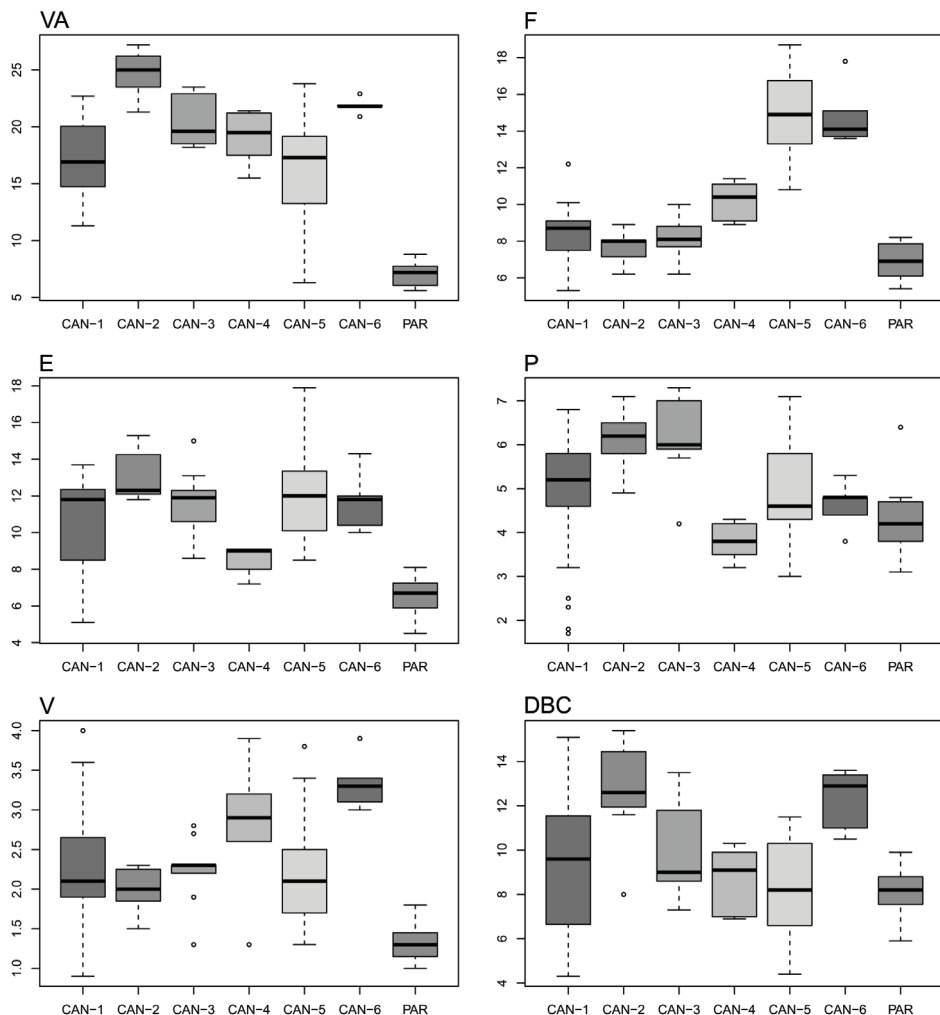


**Figure 44.** Box plots for genitalia characters of the seven *Monacha* clades investigated. The lower and upper limits of the rectangular boxes indicate the 25<sup>th</sup> to 75<sup>th</sup> percentile range, and the horizontal line within the boxes is the median (50<sup>th</sup> percentile).

pairs, respectively). The most recognizable pairs were CAN-5 vs PAR or CAN-6 vs PAR (four significant characters), CAN-1 vs PAR or CAN-4 vs PAR (3 significant characters) and CAN-2 vs CAN-5, CAN-2 vs PAR or CAN-3 vs PAR (2 significant characters). Only one significant character distinguished CAN-1 vs CAN-2, CAN-1 vs CAN-5, CAN-1 vs CAN-6, CAN-2 vs CAN-6, CAN-3 vs CAN-5, CAN-3 vs CAN-6, CAN-4 vs CAN-5 or CAN-4 vs CAN-6 and none distinguished CAN-1 vs CAN-3, CAN-1 vs CAN-4, CAN-2 vs CAN-3, CAN-2 vs CAN-4, CAN-3 vs CAN-4 or CAN-5 vs CAN-6 (Table 6).



## Discussion

Pieńkowska et al. (2018) found that *M. cantiana*, as usually conceived, actually consists of four distinct lineages (CAN-1, CAN-2, CAN-3 and CAN-4). Examination of a group of four additional populations from the Apuan Alps revealed two more lineages (CAN-5 and CAN-6). From a molecular point of view, they are quite distinct from each other and from all the others but from a morphological point of view they are indistinguishable from each other and only slightly distinguishable from the others.

Our present results confirm that lineages CAN-1, CAN-2 and CAN-3 can be distinguished by analysis of mitochondrial gene (COI and 16SrDNA) sequences (Figs 1, 4, 5) but not by nuclear gene (H3 and ITS2) sequences (Fig. 2). On the other hand, analysis of both nucleotide sequences (of mitochondrial and nuclear genes) showed that the CAN-4, CAN-5 and CAN-6 lineages are distinct from all the others (Figs 1–3). Moreover, these gene sequences clearly separated *M. cantiana* lineages from *M. parumcincta*.

Based on their studies of lepidopteran relationships, Hebert et al. (2003a, b) suggested that nucleotide sequences of the mitochondrial COI gene could be a universal tool for species distinction. This so called “barcode method” has since been widely used (Tautz et al. 2003; Hebert et al. 2004, 2013; Hajibabaei et al. 2007; Packer et al. 2009; Goldstein and Desalle 2011; Čandek and Kuntner 2015; Dabert et al. 2018; Yang et al. 2018, but see e.g.: Moritz and Cicero 2004; Taylor and Harris 2012). It has also been used to solve taxonomic problems in different gastropod families (Hershler et al. 2003; Remigio and Hebert 2003; Rundell et al. 2004; Elejalde et al. 2008; Duda et al. 2011; Delicado et al. 2012; Breugelmans et al. 2013; Proćków et al. 2013, 2014). However, a 3% threshold was established arbitrarily by Hebert et al. (2003a, b) as a marker of species distinction, and in several stylommatophoran families it proves to be much higher (Davison et al. 2009; Sauer and Hausdorf 2010, 2012; Scheel and Hausdorf 2012). Moreover, we have always stressed (Pieńkowska et al. 2015, 2018) that molecular features alone are insufficient to define species but need to be supported by anatomical features.

In light of the above, we underline that the interspecific genetic distances in COI sequences between both, CAN-5 and CAN-6, and all other lineages of *M. cantiana* s.l. (CAN-5 vs CAN-1/CAN-2/CAN-3/CAN-4 – 13.3–18.2%, CAN-6 vs CAN-1/CAN-2/CAN-3/CAN-4 – 14.3–19.2%; Table 5) are an order of magnitude greater than Hebert’s 3% threshold (Hebert et al. 2003a, b). It is also an order of magnitude greater than intraspecific divergence (“barcode gap”, see Hebert et al. 2004; Čandek and Kuntner 2015) within CAN-5 and CAN-6 lineages, 1.3% and 1.6%, respectively (Table 5). The analysis of mitochondrial COI and 16SrDNA sequences (Figs 1, 4, 5) are supported by the results of nuclear ITS2 and H3 sequences (Fig. 2). This suggests that CAN-5 and CAN-6 lineages taken together create a taxon separate from the other lineages of *M. cantiana* s.l. Despite CAN-5 differs from CAN-6 at a similarly high level (COI 12.4–14.3%) there are no morphological differences between specimens of both lineages. The speciation of CAN-5 and CAN-6 lineages therefore seems to emerge more promptly in molecular (mitochondrial gene sequences) than in morphological (shell, genitalia) features, probably because of a rapidly evolving mitochon-

**Table 7.** The best discriminant morphological characters distinguishing *Monacha cantiana* lineages (UD umbilicus diameter, F flagellum length).

		CAN-1	CAN-2	CAN-3	CAN-4	CAN-5	CAN-6	PAR
UD	mean ± S.D.	1.2 ± 0.4	1.3 ± 0.2	1.2 ± 0.4	1.0 ± 0.1	1.9 ± 0.5	2.6 ± 0.4	0.0 ± 0.0
	Range	0.3–2.0	1.1–1.6	0.8–1.9	0.8–1.1	1.1–2.8	2.2–3.1	0.0–0.0
	number of specimens	28	4	9	5	15	5	12
F	mean ± S.D.	8.5 ± 1.5	7.6 ± 1.0	8.0 ± 1.2	10.2 ± 1.1	14.9 ± 2.5	14.9 ± 1.7	6.9 ± 1.0
	range	5.3–12.2	6.2–8.9	6.2–10.0	8.9–11.4	10.8–18.7	13.6–17.8	5.4–8.2
	number of specimens	23	7	9	5	15	5	11

All dimensions in mm.

drial genome (Thomaz et al. 1996; Remigio and Hebert 2003). As mentioned above, molecular data alone cannot be used to distinguish species. It must be supported by morphological features of shells and/or genital anatomy before any decision is made about taxonomy or nomenclature.

Statistical analysis of 12 shell and six anatomical characters showed that CAN-5 and CAN-6 cannot be distinguished from each other by morphology (no character shows statistically significant differences according to Tukey's honestly significant difference test). They are only marginally distinct from CAN-1, CAN-2, CAN-3 and CAN-4, but clearly distinct from *M. parumcincta*, used for comparison: two or three characters distinguish the group CAN-5 plus CAN-6 from CAN-1, CAN-2 and CAN-3; one character distinguishes CAN-5 from CAN-4; five characters distinguish CAN-6 from CAN-4; 11–14 characters distinguish the group CAN-5 plus CAN-6 from PAR. It is possible that the small sample available for lineages CAN-4 and CAN-6 (one population for each) biased comparison of these two lineages. The best discriminant characters separating the group CAN-5 plus CAN-6 from all the other lineages are umbilicus diameter (UD) and flagellum length (F). In both cases the lineages CAN-5 and CAN-6 have the highest values (Table 7).

As in the case of other lineages, the greatest bias of morphological analysis was the small sample available for lineages CAN-2, CAN-3, CAN-4 and CAN-6, which prevented a realistic account of their variability. As far as we know, this newly recognised group only occurs in the Apuan Alps and consists of two differentiated lineages (CAN-5 and CAN-6). Although examination of additional populations is desirable, intra-Apuan differentiation is also known for other organisms such as plants (Bedini et al. 2011) and animals (Zinetti et al. 2013).

Six available names have been introduced for *Monacha cantiana* s.l. from north-western Tuscany (see Appendix 1). The oldest, *Helix anconae*, was established by Issel (1872) for specimens reported from a wide area extending northward to Arenzano in Liguria and southward to island of Elba and the Maremma of Tuscany. However, all the localities quoted are in coastal and lowland Liguria and Tuscany, while the populations including the group CAN-5 plus CAN-6 are from mountain sites. This would exclude a relationship of this nominal taxon with these lineages.



**Figures 45–47.** Syntypes and original labels of *Monacha* species from Apuan Alps established by Mabilles (1881). *Helix apuanica* (45) (MHNG-MOLL-115981), *Helix ardesa* (46) (MHNG-MOLL-115982), *Helix sobara* (47) (MHNG-MOLL-116022) (by courtesy of E. Tardy, Muséum d'histoire naturelle, Genève, Switzerland).

All the other names were established by Mabilles (1881) and De Stefani (1883–1888) for specimens collected in the Apuan Alps. Syntypes of the three nominal taxa introduced by Mabilles (1881) are in Bourguignat's collection at the Muséum d'histoire naturelle, Genève (Switzerland) (Figs 45–47). Syntypes of the two nominal taxa established by De Stefani (1883–1888) are not known and probably lost. Umbilicus diameter of the shells of the syntypes of Mabilles's species and the specimens illustrated by De Stefani is consistent for at least five of these nominal taxa with that of *Monacha* of the group CAN-5 plus CAN-6 (*Helix sobara* Mabilles, 1881, *Helix ardesa* Mabilles, 1881, *Helix apuanica* Mabilles, 1881, *Helix carfaniensis* De Stefani, 1883 and *Helix spallanzanii* De Stefani, 1884). Mabilles's three nominal taxa have precedence over those of De Stefani, and because the former were published simultaneously in the same paper, their relative precedence can only be determined by the first revisor (ICZN 1999: Art. 24). Although all three match *Monacha* of the group CAN-5 plus CAN-6, the best correspondence is

with *Helix sobara*. Nevertheless, the availability of these names for the lineages CAN-5 and CAN-6 is somewhat difficult and not immediate. These nominal taxa were only established on shell characters, but no shell character shows statistically significant differences between CAN-5 and CAN-6. Their relationships could only therefore be established by molecular study of topotypes, but unfortunately Mabille (1881) did not quote any precise collection site. In some cases, the identity and relationships of extinct taxa have been addressed and clarified through study of ancient DNA from dried tissue (e.g. Villanea et al. 2016; Vogler et al. 2016). Unfortunately, this approach is not applicable for Mabille's syntypes because they consist only of shells devoid of any dried tissue. Thus, the case can only be solved by appeal to article 75.5 of the Code (ICZN 1999).

However, before proposing a definitive nomenclatural taxonomic setting, it is necessary to examine other populations of the group. In the meantime, these lineages should continue to be defined informally, in order to avoid creating settings based on partial and insufficient data. This approach has also been used for other gastropods, such as *Carychium minimum* Müller, 1774 and *Carychium tridentatum* (Risso, 1826) (see Weigand et al. 2012), *Ancylus fluviatilis* (Müller, 1774) (see Pfenninger et al. 2003; Albrecht et al. 2006) and *Rumina decollata* (Linnaeus, 1758) (see Prévot et al. 2016).

## Acknowledgements

We are grateful to Michael Duda (Naturhistorisches Museum Wien, Austria) for providing specimens. We thank Helen Ampt (Siena, Italy) for revising the English, Giovanni Cappelli (Siena, Italy) for taking photographs of shells, Emmanuel Tardy (Muséum d'histoire naturelle, Genève, Switzerland) for providing information and photos of Mabille's syntypes in Bourguignat's collection. Many thanks also to Robert AD Cameron (University of Sheffield, United Kingdom) and to Bernhard Hausdorf (University of Hamburg, Germany) for their valuable comments on the manuscript.

## References

- Albrecht C, Trajanovski S, Kuhn K, Streit B, Wilke T (2006) Rapid evolution of an ancient lake species flock: freshwater limpets (Gastropoda: Ancyliidae) in the Balkan Lake Ohrid. *Organisms Diversity & Evolution* 6: 294–307. <https://doi.org/10.1016/j.ode.2005.12.003>
- Alzona C (1971) Malacofauna italica. Catalogo e bibliografia dei Molluschi viventi, terrestri e d'acqua dolce. *Atti della Società Italiana di Scienze Naturali e del Museo Civico di Storia Naturale di Milano* 111: 1–433.
- Bandelt H-J, Forster P, Röhl A (1999) Median-joining networks for inferring intraspecific phylogenies. *Molecular Biology Evolution* 16: 37–48. <https://doi.org/10.1093/oxfordjournals.molbev.a026036>
- Bedini G, Carta A, Zecca G, Grassi F, Casazza G, Minuto L (2011) Genetic structure of *Rhamnus glaucophylla* Sommier endemic to Tuscany. *Plant Systematics and Evolution* 294: 273–280. <https://doi.org/10.1007/s00606-011-0469-4>

- Biondi M, Urbani F, D'Alessandro P (2013) Endemism patterns in the Italian leaf beetle fauna (Coleoptera, Chrysomelidae). *ZooKeys* 332: 177–205. <https://doi.org/10.3897/zookeys.332.5339>
- Breugelmans K, Jordaens K, Adriaens E, Remon JP, Cardona JQ, Backeljau T (2013) DNA barcodes and phylogenetic affinities of the terrestrial slugs *Arion gilvus* and *A. ponsi* (Gastropoda, Pulmonata, Arionidae). *ZooKeys* 365: 83–104. <https://doi.org/10.3897/zookeys.365.6104>
- Cadahia L, Harl J, Duda M, Sattmann H, Kruckenhausner L, Feher Z, Zopp L, Haring E (2014) New data on the phylogeny of Ariantinae (Pulmonata, Helicidae) and the systematic position of *Cylindrus obtusus* based on nuclear and mitochondrial DNA marker sequences. *Journal of Zoological Systematics and Evolutionary Research* 52: 163–169. <https://doi.org/10.1111/jzs.12044>
- Carta A, Pierini B, Roma-Marzio F, Bedini G, Peruzzi L (2017) Phylogenetic measures of biodiversity uncover pteridophyte centres of diversity and hotspots in Tuscany. *Plant Biosystems* 152: 831–839. <https://doi.org/10.1080/11263504.2017.1353550>
- Castresana J (2000) Selection of conserved blocks from multiple alignments for their use in phylogenetic analysis. *Molecular Biology and Evolution* 17: 540–552. <https://doi.org/10.1093/oxfordjournals.molbev.a026334>
- Čandek K, Kuntner M (2015) DNA barcoding gap: reliable species identification over morphological and geographical scales. *Molecular Ecology Resources* 15: 268–277. <https://doi.org/10.1111/1755-0998.12304>
- Dabert J, Mironov SV, Janiga M (2018) Two new species of the feather mite genus *Analgus* Nitzsch, 1818 (Analgoidea: Analgidae) from accentors (Passeriformes: Prunellidae) — morphological descriptions with DNA barcode data. *Systematic and Applied Acarology* 23: 2288–2303. <https://doi.org/10.11158/saa.23.12.2>
- Darriba D, Taboada GL, Doallo R, Posada D (2012) jModelTest 2: more models, new heuristics and parallel computing. *Nature Methods* 9: 772. <https://doi.org/10.1038/nmeth.2109>
- Davison A, Blackie RL, Scothern GP (2009) DNA barcoding of stylommatophoran land snail: a test of existing sequences. *Molecular Ecology Resources* 9: 1092–1101. <https://doi.org/10.1111/j.1755-0998.2009.02559x>
- Delicado D, Machordom A, Ramos MA (2012) Underestimated diversity of hydrobiid snails. The case of *Pseudamnicola* (*Corrosella*) (Mollusca: Caenogastropoda: Hydrobiidae). *Journal of Natural History* 46: 25–89. <https://doi.org/10.1080/00222933.2011.623358>
- De Stefani C (1883–1888) Molluschi viventi nelle Alpi Apuane nel Monte Pisano e nell'Apennino adiacente. *Bullettino della Società Malacologica Italiana* 9 (1–5): 11–80 (1883), 9 (6–12): 81–192 (1883), 9 (13–19): 193–253 (1884), 13 (11–13): figs 1–32 [1–2] (1888).
- Duda M, Sattmann H, Haring E, Bartel D, Winkler H, Harl J, Kruckenhausner L (2011) Genetic differentiation and shell morphology of *Trochulus oreinos* (Wagner, 1915) and *T. hispidus* (Linnaeus, 1758) (Pulmonata: Hygromiidae) in the northeastern alps. *Journal of Molluscan Studies* 77: 30–40. <https://doi.org/10.1093/mollus/eqy037>
- Elejalde MA, Madeira MJ, Muñoz B, Arrébola JR, Gómez-Moliner BJ (2008) Mitochondrial DNA diversity and taxa delineation in the land snails of the *Iberus gualterianus* (Pulmonata, Helicidae) complex. *Zoological Journal of the Linnean Society* 154: 722–737. <https://doi.org/10.1111/j.1096-3642.2008.00427.x>
- Felsenstein J (1985) Confidence limits on phylogenies: an approach using the bootstrap. *Evolution* 39: 783–791. <https://doi.org/10.2307/2408678>



- Garbari F, Bedini G (2014) The flora of the Apuan Alps (Tuscany, Italy): survey of biosystematic investigations. *Willdenowia* 36: 149–155. <https://doi.org/10.3372/wi.36.36112>
- Glez-Peña D, Gómez-Blanco D, Reboiro-Jato M, Fdez-Riverola F, Posada D (2010) ALTER: program-oriented format conversion of DNA and protein alignments. *Nucleic Acids Research* 38 (Web Server issue): W14–W18. <https://doi.org/10.1093/nar/gkq321>
- Goldstein PZ, DeSalle R (2011) Integrating DNA barcode data and taxonomic practice: determination, discovery, and description. *BioEssays* 33: 135–147. <https://doi.org/10.1002/bies.201000036>
- Hajibabaei M, Singer GAC, Clare EL, Hebert PDN (2007) Design and applicability of DNA arrays and DNA barcodes in biodiversity monitoring. *BMC Biology* 5: 24. <https://doi.org/10.1186/1741-7007/5/24>
- Hall TA (1999) BioEdit: a user friendly biological sequence alignment editor and analysis program for Windows 95/98/NT. *Nucleic Acids Symposium Series* 41: 95–98. <http://brownlab.mbio.ncsu.edu/JWB/papers/1999Hall1.pdf>
- Hasegawa M, Kishino H, Yano T (1985) Dating the human-ape split by a molecular clock of mitochondrial DNA. *Journal of Molecular Evolution* 22: 160–174. <https://doi.org/10.1007/BF02101694>
- Hebert PDN, Cywinska A, Ball SL, deWaard JR (2003a) Biological identifications through DNA barcodes. *Proceedings of the Royal Society B: Biological Sciences* 270: 313–321. <https://doi.org/10.1098/rspb.2002.2218>
- Hebert PDN, deWaard JR, Zakharov EV, Prosser SWJ, Sones JE, McKeown JAT, Mantle B, LaSalle J (2013) DNA ‘barcode blitz’: rapid digitization and sequencing of a natural history collection. *PLoS One* 8: e68535. <https://doi.org/10.1371/journal.pone.0068535>
- Hebert PDN, Ratnasingham S, deWaard JR (2003b) Barcoding animal life: cytochrome c oxidase subunit 1 divergences among closely related species. *Proceedings of the Royal Society B: Biological Sciences* 270 (Suppl. 1): 596–599. <https://doi.org/10.1098/rsbl.2003.0025>
- Hebert PDN, Stoeckle MY, Zemplak TS, Francis CM (2004) Identification of birds through DNA barcodes. *PLoS Biology* 10: e312 (1657–1663). <https://doi.org/10.1371/journal.pbio.0020312>
- Hershler R, Liu HP, Thompson FG (2003) Phylogenetic relationships of North American nymphophiline gastropods based on mitochondrial DNA sequences. *Zoologica Scripta* 32: 357–366. <https://doi.org/10.1046/j.1463-6409.2003.00115.x>
- ICZN (International Commission on Zoological Nomenclature) (1999) *International Code of Zoological Nomenclature*, 4th Edition. The International Trust for Zoological Nomenclature, London, 306 pp.
- Issel A (1872) Appendice al Catalogo dei Molluschi raccolti nella provincia di Pisa. *Atti della Società Italiana di Scienze Naturali* 15: 58–76.
- Kimura M (1980) A simple method for estimating evolutionary rate of base substitutions through comparative studies of nucleotide sequences. *Journal of Molecular Evolution* 16: 111–120. <https://doi.org/10.1007/bf01731581>
- Kruckenhauser L, Duda M, Bartel D, Sattmann H, Harl J, Kirchner S, Haring E (2014) Paraphyly and budding speciation in the hairy snail (Pulmonata, Hygromiidae). *Zoologica Scripta* 43: 273–288. <https://doi.org/10.1111/zsc.12046>

- Kumar S, Stecher G, Tamura K (2016) MEGA7: Molecular Evolutionary Genetics Analysis version 7.0 for bigger datasets. *Molecular Biology and Evolution* 33: 1870–1874. <https://doi.org/10.1093/molbev/msw054>
- Lanza B (1997) La fauna endemica delle Alpi Apuane (Toscana, Italia). *Atti della Società Toscana di Scienze Naturali Residente in Pisa Memorie Serie B* 103: 17–37.
- Linnaeus C (1758) *Systema naturæ per regna tria naturæ, secundum classes, ordines, genera, species, cum characteribus, differentiis, synonymis, locis*. Editio decima, reformata. Tomus I. Salvius, Holmiæ, 4 + 824 pp.
- Mabille J (1881) Testarum novarum præsertim europæarum diagnoses. *Bulletin de la Société Philomathique de Paris Septième Série* 5: 122–130. <https://www.biodiversitylibrary.org/item/98733#page/136>
- Manganelli G, Salomone N, Giusti F (2005) A molecular approach to the phylogenetic relationships of the western palæarctic Helicoidea (Gastropoda: Stylommatophora). *Biological Journal of Linnean Society London* 85: 501–512. <https://doi.org/10.1111/j.1095-8312.2005.00514.x>
- Montagu G (1803) *Testacea Britannica, or, Natural history of British shells, marine, land, and fresh-water, including the most minute: systematically arranged and embellished with figures*. 2 vols, Romsey, London, xxxvii + 606 pp.
- Moritz C, Cicero C (2004) DNA barcoding: promise and pitfalls. *PLoS Biology* 2(10): e354. <https://doi.org/10.1371/journal.pbio.0020354>
- Müller OF (1774) *Vermium terrestrium et fluviatilium, seu animalium infusorium, helminthicorum, et testaceorum, non marinorum, succinct historia*. Vol. II. Heineck & Faber, Havniae et Lipsiae, xxxvi + 214 + 10 pp.
- Nei M, Kumar S (2000) *Molecular Evolution and Phylogenetics*. Oxford University Press, New York, 352 pp.
- Neiber MT, Hausdorf B (2015) Phylogeography of the land snail genus *Circasina* (Gastropoda: Hygromiidae) implies multiple Pleistocene refugia in the western Caucasus region. *Molecular Phylogenetics and Evolution* 93: 129–142. <https://doi.org/10.1016/j.ympev.2015.07.012>
- Orsenigo S, Montagnani C, Fenu G, Gargano D, Peruzzi L, Abeli T, Alessandrini A, Bacchetta G, Bartolucci F, Bovio M, Brullo C, Brullo S, Carta A, Castello M, Cogoni D, Conti F, Domina G, Foggi B, Gennai M, Gigante D, Iberite M, Lasen C, Magrini S, Perrino EV, Prosser F, Santangelo A, Selvaggi A, Stinca A, Vagge I, Villani M, Wagensommer R, Wilhalm T, Tartaglini N, Duprè E, Blasi C, Rossi G (2018) Red Listing plants under full national responsibility: extinction risk and threats in the vascular flora endemic to Italy. *Biological Conservation* 224: 213–222. <https://doi.org/10.1016/j.biocon.2018.05.030>
- Packer L, Grixti JC, Roughley RE, Hanner R (2009) The status of taxonomy in Canada and the impact of DNA barcoding. *Canadian Journal of Zoology* 87: 1097–1110. <https://doi.org/10.1139/Z09-100>
- Pfenninger M, Staubach S, Albrecht C, Streit B, Schwenk K (2003) Ecological and morphological differentiation among cryptic evolutionary lineages in freshwater limpets of the nominal form-group *Ancylus fluviatilis* (O.F. Müller 1774). *Molecular Ecology* 12: 2731–2745. <https://doi.org/10.1046/j.1365-294X.2003.01943.x>

- Pieńkowska JR, Giusti F, Manganelli G, Lesicki A (2015) *Monacha claustralis* (Rossmässler 1834) new to Polish and Czech malacofauna (Gastropoda: Pulmonata: Hygromiidae). *Journal of Conchology* 42: 79–93.
- Pieńkowska JR, Lesicki A (2018) A note on status of *Galba occulta* Jackiewicz, 1959 (Gastropoda: Hygrophila: Lymnaeidae). *Folia Malacologica* 26: 231–247. <https://doi.org/10.12657/fofmal.026.029>
- Pieńkowska JR, Manganelli G, Giusti F, Hallgass A, Lesicki A (2018) Exploring *Monacha cantiana* (Montagu, 1803) phylogeography: cryptic lineages and new insights into the origin of the English populations (Eupulmonata, Stylommatophora, Hygromiidae). *ZooKeys* 765: 1–41. <https://doi.org/10.3897/zookeys.765.24386>
- Prévot V, Jordaens K, Sonet G, Backeljau T (2013) Exploring species level taxonomy and species delimitation methods in the facultatively self-fertilizing land snail genus *Rumina* (Gastropoda: Pulmonata). *PLoS One* 8(4): e60736. <https://doi.org/10.1371/journal.pone.0060736>
- Proćków M, Mackiewicz P, Pieńkowska JR (2013) Genetic and morphological studies of species status for poorly known endemic *Trochulus phorochaetius* (Bourguignat, 1864) (Gastropoda: Pulmonata: Hygromiidae), and its comparison with closely related taxa. *Zoological Journal of Linnean Society* 169: 124–143. <https://doi.org/10.1111/zoj.12048>
- Proćków M, Strzała T, Kuźnik-Kowalska E, Mackiewicz P (2014) Morphological similarity and molecular divergence of *Trochulus striolatus* and *T. montanus*, and their relationship to sympatric congeners (Gastropoda: Pulmonata: Hygromiidae). *Systematics and Biodiversity* 12: 366–384. <https://doi.org/10.1080/14772000.2014.925986>
- Razkin O, Gomez-Moliner BJ, Prieto CE, Martinez-Orti A, Arrebola JR, Munoz B, Chueca LJ, Madeira MJ (2015) Molecular phylogeny of the western Palaearctic Helicoidea (Gastropoda, Stylommatophora). *Molecular Phylogenetics and Evolution* 83: 99–117. <https://doi.org/10.1016/j.ympev.2014.11.014>
- Remigio EA, Hebert PDN (2003) Testing the utility of partial COI sequences for phylogenetic estimates of gastropod relationships. *Molecular Phylogenetics and Evolution* 29: 641–647. [https://doi.org/10.1016/S1055-7903\(03\)00140-4](https://doi.org/10.1016/S1055-7903(03)00140-4)
- Risso A (1826) Histoire naturelle des principales productions de l'Europe méridionale et particulièrement de celles des environs de Nice et des Alpes Maritimes. Tome quatrième. Levrault, Paris, 10 + 439 + 12 pp. <https://doi.org/10.5962/bhl.title.58984>
- Ronquist F, Huelsenbeck JP (2003) MRBAYES 3: Bayesian phylogenetic inference under mixed models. *Bioinformatics* 19: 1572–1574. <https://doi.org/10.1093/bioinformatics/btg180>
- Rossmässler EA (1834) Diagnoses conchyliorum terrestrium et fluviatilium. Zugleich zu Fascikeln natürlicher Exemplare. II Heft. No. 21–40. Arnold, Dresden & Leipzig, 8 pp. <https://doi.org/10.5962/bhl.title.10380>
- Rundell RJ, Holland BS, Cowie RH (2004) Molecular phylogeny and biogeography of the endemic Hawaiian Succineidae (Gastropoda: Pulmonata). *Molecular Phylogenetics and Evolution* 31: 246–255. <https://doi.org/10.1016/j.ympev.2003.07.014>
- Saitou N, Nei M (1987) The neighbor-joining method: A new method for reconstructing phylogenetic trees. *Molecular Biology and Evolution* 4: 406–425. <https://doi.org/10.1093/oxfordjournals.molbev.a040454>



- Sauer J, Hausdorf B (2010) Reconstructing the evolutionary history of the radiation of the land snail genus *Xerocrassa* on Crete based on mitochondrial sequences and AFLP markers. *BMC Evolutionary Biology* 10: 299. <https://doi.org/10.1186/1471-2148-10-299>
- Sauer J, Hausdorf B (2012) A comparison of DNA-based methods for delimiting species in a Cretan land snail radiation reveals shortcomings of exclusively molecular taxonomy. *Cladistics* 28: 300–316. <https://doi.org/10.1111/j.1096-0031.2011.00382.x>
- Scheel BM, Hausdorf B (2010) Survival and differentiation of subspecies of the land snail *Charpentieria itala* in mountain refuges in the Southern Alps. *Molecular Ecology* 21: 3794–3808.
- Talavera G, Castresana J (2007) Improvement of phylogenies after removing divergent and ambiguously aligned blocks from protein sequence alignments. *Systematic Biology* 56: 564–577. <https://doi.org/10.1080/10635150701472164>
- Tamura K (1992) Estimation of the number of nucleotide substitutions when there are strong transition-transversion and G+C-content biases. *Molecular Biology and Evolution* 9: 678–687. <https://doi.org/10.1093/oxfordjournals.molbev.a040752>
- Tautz D, Arctander P, Minelli A, Thomas RH, Vogler AP (2003) A plea for DNA taxonomy. *Trends in Ecology & Evolution* 18: 70–74. [https://doi.org/10.1016/S0169-5347\(02\)00041-1](https://doi.org/10.1016/S0169-5347(02)00041-1)
- Taylor HR, Harris WE (2012) An emergent science on the brink of irrelevance: a review of the past 8 years of DNA barcoding. *Molecular Ecology Resources* 12: 377–388. <https://doi.org/10.1111/j.1755-0998.2012.03119.x>
- Thompson JD, Higgins DG, Gibson TJ (1994) CLUSTAL W: improving the sensitivity of progressive multiple sequence alignment through sequence weighting, position specific gap penalties and weight matrix choice. *Nucleic Acids Research* 22: 4673–4680. <https://doi.org/10.1093/nar/22.22.4673>
- Thomaz D, Guiller A, Clarke B (1996) Extreme divergence of mitochondrial DNA within species of pulmonate land snails. *Proceedings of Royal Society B: Biological Sciences* 263: 363–368. <https://doi.org/10.1098/rspb.1996.0056>
- Villanea FA, Parent CE, Kemp BM (2016) Reviving Galápagos snails: ancient DNA extraction and amplification from shells of probably extinct endemic land snails. *Journal of Molluscan Studies* 82: 449–456. <https://doi.org/10.1093/mollus/eyw011>
- Vogler RE, Beltramino AA, Strong EE, Rumi A, Peso JG (2016) Insights into the evolutionary history of an extinct South American freshwater snail based on historical DNA. *PLoS One* 11 (12): e0169191. <https://doi.org/10.1371/journal.pone.0169191>
- Weigand AM, Pfenninger M, Jochum A, Klussmann-Kolb A (2012) Alpine crossroads or origin of genetic diversity? Comparative phylogeography of two sympatric microgastropod species. *PLoS One* 7 (5): e37089. <https://doi.org/10.1371/journal.pone.0037089>
- Yang QQ, Liu SW, Yu XP (2018) Research progress on DNA barcoding analysis methods. *Ying Yong Sheng Tai Xue Bao (Chinese Journal of Applied Ecology)* 29: 1006–1014. [in Chinese with English abstract]
- Zinetti F, Dapporto L, Vanni S, Magrini P, Bartolozzi L, Chelazzi G, Ciofi C (2013) Application of molecular genetics and geometric morphometrics to taxonomy and conservation of cave beetles in central Italy. *Journal of Insect Conservation* 17: 921–932. <https://doi.org/10.1007/s10841-013-9573-9>

## Appendix I

### Nominal taxa of *Monacha cantiana* group established from north-western Tuscany

#### *Helix anconae* Issel, 1872: 63–65

Type locality: “[...] Montecatini, Val di Nievole, non lungi da Cecina nella Maremma toscana, nell’isola d’Elba, a Genova, ad Arenzano ed in altre località della Toscana e della Liguria.”

Type material: probably lost.

Status: listed as subspecies of *Monacha cantiana* by Alzona (1971).

#### *Helix sobara* Mabille, 1881: 126–127

Type locality: “in Alpibus Apuanis.”

Type material: one syntype (MHNG-MOLL-116022) is in Bourguignat’s collection at Muséum d’histoire naturelle, Genève (Switzerland).

Note: assigned to J. Bourguignat.

Status: listed as junior synonym of *Monacha cantiana anconae* by Alzona (1971).

#### *Helix ardesa* Mabille, 1881: 127

Type locality: “in Alpibus Apuanis.”

Type material: one syntype (MHNG-MOLL-115982) is in Bourguignat’s collection at Muséum d’histoire naturelle, Genève (Switzerland).

Note: assigned to J. Bourguignat.

Status: listed as junior synonym of *Monacha cantiana anconae* by Alzona (1971).

#### *Helix apuanica* Mabille, 1881: 127–128

Type locality: “in Alpibus Apuanis.”

Type material: one syntype (MHNG-MOLL-115981) is in Bourguignat’s collection at Muséum d’histoire naturelle, Genève (Switzerland).

Note: assigned to J. Bourguignat.

Status: listed as junior synonym of *Monacha cantiana anconae* by Alzona (1971).

#### *Helix (Monacha) carfaniensis* De Stefani, 1883: 53–54 (as “*Helix carfaniensis*”), 1884: 231, 1888: fig. 8.

Type locality: Serchio Valley, Vagli. De Stefani (1884: 231) stated that the type is from Serchio Valley and depicted a shell from Vagli.

Type material: probably lost.

Status: listed as junior synonym of *Monacha cantiana anconae* by Alzona (1971).

#### *Helix (Monacha) carfaniensis* subvar. *minor* De Stefani, 1883: 54 (as “subvar. *minor*”)

Type locality: “App[ennino]. San Pellegrino 1464 [m].”

Type material: probably lost.

Note: First reported by De Stefani (1875: 43–44) as *Helix cantiana* var. *minor* Albers.

Status: not available because this name denotes an infrasubspecific taxon.

***Helix (Eulota) cemelelea forma isselii*** De Stefani, 1883: 55–59 (as “*Helix cemelelea* forma *isselii*”)

Type locality: see *Helix spallanzanii* below.

Type material: probably lost.

Status: not available because junior homonym of *Helix isseli* Morelet, 1872; re-named as *Helix spallanzanii* De Stefani, 1884.

***Helix spallanzanii*** De Stefani, 1884: 208, 231, 1888: fig. 7.

Type locality: Apuan Alps, Vagli. De Stefani (1884: 231) stated that the type is from Apuan Alps and depicted a shell from Vagli.

Type material: probably lost.

Status: new name for *Helix (Eulota) cemelelea* forma *isselii* De Stefani, 1883, junior homonym of *Helix isseli* Morelet, 1872.

Status: listed as junior synonym of *Monacha cantiana anconae* by Alzona (1971).